LATERAL STEERING OF THE WEB IN A DIFFERENTIALLY LOADED NIP OF RUBBER COVERED ROLLERS

By

KAVITHA BALAIYAN

Bachelor of Science

Anna University,

Tamil Nadu, India

2000

Submitted to the Faculty of the Graduate College of
the Oklahoma State University in partial fulfillment
of the requirements for the Degree of
MASTER OF SCIENCE
December, 2005

LATERAL STEERING OF THE WEB IN

A DIFFERENTIALLY LOADED NIP OF

RUBBER COVERED ROLLERS

Thesis Approved:

Dr. James Keith Good

Thesis Advisor

Dr. Gary E. Young

Dr. Christopher Eric Price

Dr. A. Gordon Emslie

Dean of the Graduate College

ACKNOWLEDGEMENTS

I would like to express my heartfelt gratitude to my advisor and mentor Dr.James Keith Good. Without his able guidance and encouragement, this research project would not have become a reality. He has been very patient, considerate and helpful throughout this project. I'm grateful to Dr.Good for giving me an opportunity to work at the Web Handling Research Center. I highly regard and treasure the experience of working with him.

I would like to thank my committee members, Dr. Christopher Eric Price and Dr. Gary Young for their valuable time and support. I'm thankful to Dr.Price for inculcating a professional outlook into me. The experience of being his student has kindled an urge in me to be technically up-to-date and progressive in life. I'm highly grateful to him for that. I would also like to thank Dr.Young for his constant advice and help.

I wish to express my gratefulness to all my friends. My sincere appreciation goes to Melwin Thomas for his care and concern. He has always been a great motivator. I'm highly grateful to Paraneetharan and Krishnan, who have always extended their moral support whenever I was in need.

I would like to express my deepest sense of gratitude to my parents Mr.Balaiyan and Mrs. Thavamani and my brothers Gowtham and Ezhilarasan. Without their love and prayers, my Graduate studies and this project would not have become possible.

TABLE OF CONTENTS

LIST OF TABLES

LIST OF FIGURES

NOMENCLATURE

a	Half contact width
A	a constant
C	a constant
E_0	Modulus of elasticity of rubber as a function of hardness and strain rate
E_c	Modulus of elasticity of rubber as a function of hardness, strain rate and temperature
E_{con}	Modulus of elasticity of rubber including the confinement effects
E_{web}	Modulus of elasticity of the web
f	Load acting on a finite element
F	Load
I	Moment of inertia
IRHD	International Rubber Hardness Degree (equivalent to Shore A)
k	Material parameter for rubber
K	a variable, $(a/2t)$
KK_{web}	a parameter, constant for the given operating conditions in the web deflection expression $\left(\sqrt{T/E_c I}\right)$
KK_{sweb}	Specific Stiffness of the web
L	Length of the web prior to the nip
M	Moment

p	Contact Pressure
R	Nominal roller radius
S	Shape factor for rubber
t	Thickness of the rubber cover
T	Tension in the web
u	Radial deformation of the rubber
v	Nodal deflection of the finite beam element
V	Velocity
w	Width of the roller
W	Width of the web
Y	Lateral deflection of the web
Z	Stiffness of the elastic foundation element
δ	Indentation of the rubber cover due to nip load
ε	Strain
Φ	Angle formed by the area displaced by the nip action (chapter 2)
$\overset{o}{\varepsilon}$	Strain rate
σ	Stress
ϖ	Poisson's ratio
θ	Nodal rotation of the finite beam element
Ψ	a variable

CHAPTER 1

INTRODUCTION

A web is defined as a thin, continuous sheet or strip of material. A web is very long with respect to its width and very wide with respect to its thickness. Thus the term “web” describes film, foil, paper, woven and non-woven materials in a thin continuous strip. Webs are usually stored in the form of rolls.

The term “Web handling” refers to the transport of webs through web process machines. Handling of transportation & control of webs involve guiding and steering the web without defects. Web processes include coating, laminating, slitting, splicing, calendaring, printing, cooling, drying and cleaning.

A roller is a revolving cylinder over which a web or substrate is moved for the purpose of transporting, pressing, shaping or smoothing a web. Rollers are widely used in web handling. Rollers can be either driving the web or driven by the web. The material for the roller depends on the demands of the process in which it is used.

A nip is any two rollers in contact where the contact surface is pinched or nipped between the rollers. A nip is illustrated in Figure 1-1.

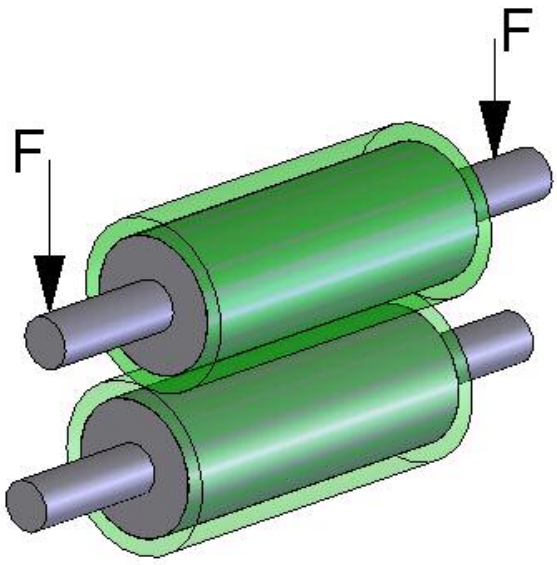

Figure 1-1: Illustration of a nip

Rubber covered nip rollers are widely used in paper, textile, sheet metal and foil processing industries and in business applications like printing, photocopying and facsimile equipments. Rubber-covered rollers have a number of applications within web-lines. They are often used to nip the web against a metal surfaced roller that is driven to achieve a certain web velocity or web tension. They are used to wring process liquids from webs. Rubber covered rollers are used commonly in other web-line processes, such as laminating two or more webs or applications involving moisture and residue removal in order to prevent contamination of downstream processes. Rubber covered nip rollers are illustrated in Figure 1-2.

Lateral movement of a web is a very important parameter in web transportation and control. Too much lateral movement can cause the formation of wrinkles and troughs. Lateral web movement can also cause the web to have

a slack edge which can impede coating or printing processes. Rubber covered rollers can induce lateral movement of a web in a process machine and thus it is important that these devices be well understood.

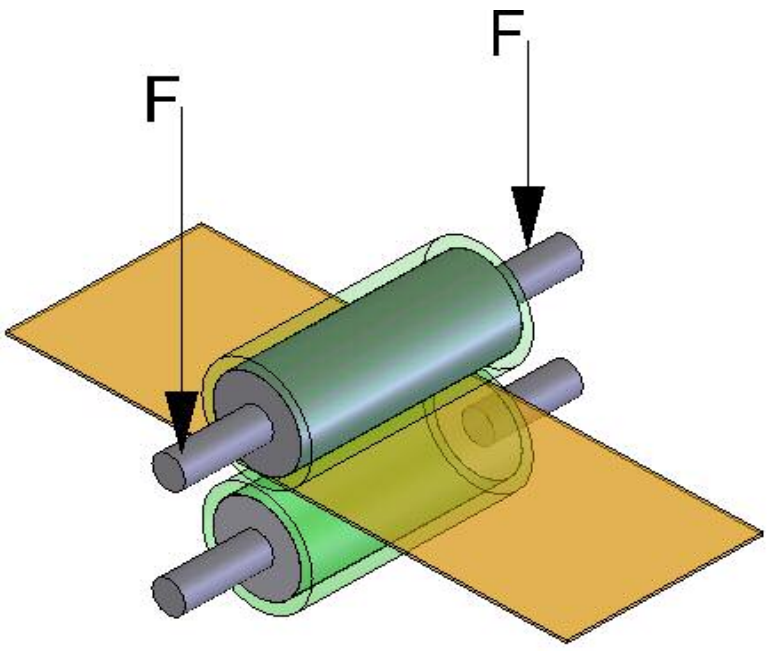

Figure 1-2: Illustration of Rubber-covered nip rollers with the web

Rubber is somewhat incompressible. If the rubber is constricted in the radial direction by impinging it with another rubber covered roller, the rubber roller will speed up in the tangential direction in the nip contact zone. This behavior can be understood with an analogy to that of the flow of an incompressible fluid through a channel of varying cross section. The mass flow rate of any fluid is the product of its density, area of cross section through which it flows and the velocity. The fluid being incompressible, there will not be any change in its volume and the density remains constant. When the liquid flows

through a constriction in the channel, the area of cross section along its path decreases and, hence, the velocity will increase in the constriction.

When a rubber covered roller is impinged by another roller, the tangential velocity of the rubber in the nip contact zone will increase. Although this is similar to the problem of the incompressible fluid moving through a constriction, it is more complex since the control volume of the rubber outside the nip contact zone has an undefined boundary.

If the nip load varies across the width of the rollers, the speed increase of the rubber will vary across the nip as well. If no slippage is assumed, this speed variation will induce a variation in the web strain across the web width. This, in turn, induces a variation in stress, giving rise to a steering moment and hence causes the lateral deformation of the web.

The objective of this research is to quantify the lateral steering of the web due to a non-uniformly loaded nip with rubber covered rollers.

CHAPTER 2

REVIEW OF LITERATURE

The behavior of rubber covered rollers has been analyzed by many authors. The situation at the nip of a rubber covered roller is illustrated in Figure 2-1. The rubber covered roller is shown to be in contact with a rigid roller. Most of the publications, on the contact between the rollers, focus on the problem assuming plane strain conditions and linear elasticity. The pressure distribution between the rollers, speed, indentation, rolling resistance, force and deformation in the nip are the widely addressed factors. The stress distributions and the tangential strains at the contact area in the nip are also addressed in some analyses.

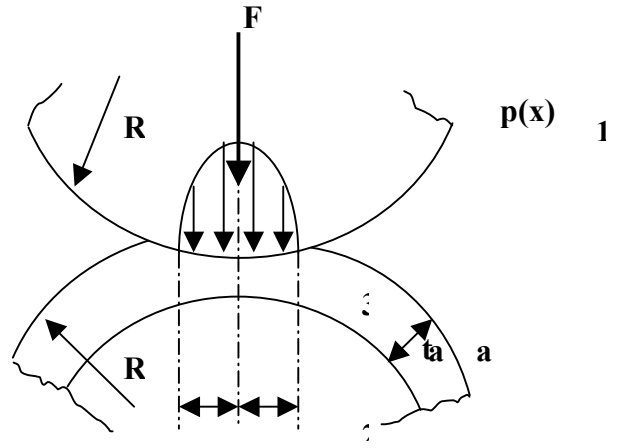

Figure 2-1: Rubber covered roller in contact with a rigid roller

An investigation of the web behavior through a nip of rubber covered rollers requires the study of the:

(a) Material Properties of rubber

(b) Relation between applied nip force and rubber cover indentation

(c) Relation between tangential strain at the nip and rubber cover indentation or nip force

(d) Relation between the tangential strain in the rubber cover and the Lateral deflection of the web

2.1 Material Properties of Rubber:

Rubber is a viscoelastic and nearly incompressible material. It is generally accepted that incompressible materials such as rubber have Poisson's ratios approaching 0.5. Hence, it calls forth interest in quantifying the elastic compression modulus and the Poisson's ratio of the material.

Good [5] found that some relationships for force vs. deformation are very sensitive to the input value of Poisson's ratio. He conducted a series of experiments and the average result of his experiments showed that the Poisson's ratio of the rubber is 0.46.

Good [4] performed compression tests on samples of Hypalon, nitrile, carboxilated nitrile, neoprene, ethylene propylene and urethane rubbers in hardness values ranging from 30 to 90 durometers (International Rubber Hardness Degree or Shore A hardness). The results proved that the Young's modulus of the rubber depends on the rubber hardness independent of the rubber type. His empirical expression for the modulus of the rubber is:

$$E_0 = 20.97\ e^{0.0564 \cdot IRHD}$$

Equation 2-1

These tests were conducted at a fixed strain rate of 0.5 in./min designated in the ASTM D575. Experimental measurements conducted at the Web Handling Research Center of Oklahoma State University have shown that rubber behaves as a viscoelastic material. Schneeburger [4] proved this by performing a large set of compression tests at various strain rates. Good [4] then developed a relation to include the effect of strain rate on elastic modulus along with rubber hardness based on this data. Good developed an empirical relation (Equation 2-2) to relate elastic modulus of rubber as a function of rubber hardness and strain rate.

$$E_0 = \left(1.6711\ \ln(\dot{\varepsilon}) + 19.51\right) \cdot e^{0.062 \cdot IRHD}$$

Equation 2-2

Kattel M. [6] studied the effect of temperature on the modulus of the rubber. The results of his experiments show that the rubber hardness decreased linearly with temperature. A new expression for the modulus of elasticity of the rubber which includes the effect of hardness, strain rate and temperature has been developed by Good [6] at the WHRC:

$$E_c = \left(1.375636\ \ln(\dot{\varepsilon}) + 29.29927\right) \cdot e^{[0.0536 \cdot (IRHD - 0.101651 \cdot (Temp - 20))]}$$

$$\left(20^0 C \le Temp \le 100^0 C\ ;\quad 30 IRHD \le IRHD \le 90 IRHD\ ;\quad 0.002\ in/in/\sec \le \dot{\varepsilon}^0 \le 0.2\ in/in/\sec\right)$$

Equation 2-3

where has the $\dot{\varepsilon}^o$ units in./in./sec and the temperature has the units of $^0 C$.

2.2 Force – Indentation Relations:

The analysis of the relation between the applied force and the cover indentation in the case of rubber covered rollers with other rollers has been addressed in various publications. Most of them are based upon elasticity solutions while some are based on empirical relations.

2.2.1 K.L. Johnson's theory:

Johnson [9] developed a relationship for nip load as a function of indentation for a rigid cylinder in contact with a cylinder having a layer of an elastic covering. Johnson assumes that the rubber cover is thin compared to the width of the roller and, hence, plane strain conditions exist.

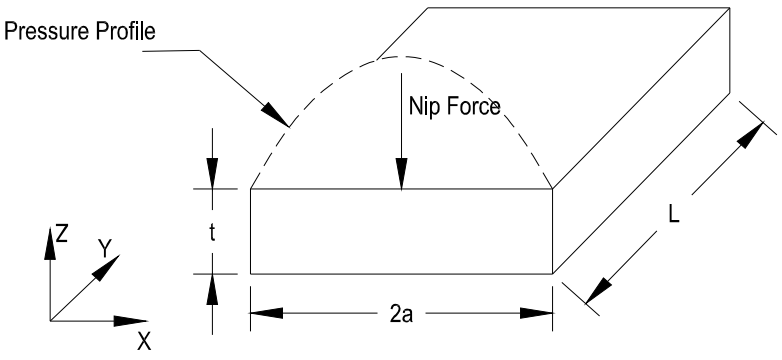

Figure 2-2: Assumption of the reacting rubber block in Johnson's model

He also assumes that the width of the contact zone is narrow compared to the diameter of the covered roller. This allowed him to assume that the nip load was reacted by a block of rubber whose dimensions would be the contact width in the horizontal ('x') direction, thickness of the rubber cover in the vertical ('z') direction and the width of the rubber covered rollers in the third ('z') direction . If the nip load has dimensions of force per unit width, then the width of the rubber roller dimension would become a unit width.

The strain in the vertical direction (ε_z) is related to the stress in the vertical direction (σ_z) and the strain in the horizontal direction (σ_x) as per the expression:

$$\varepsilon_z = \frac{1-\nu^2}{E_c}\sigma_z - \frac{\nu(1+\nu)}{E_c}\sigma_x$$

Equation 2-4

The stress in the z direction is assumed to be constant throughout the cover thickness and is equal to the contact pressure p(x). Hence,

$$\varepsilon_z = \frac{1-\nu^2}{E_c}\left[-p(x) - \frac{\nu}{1-\nu}\sigma_x\right]$$

Equation 2-5

The indentation is maximum at the center of the contact zone and is assumed to decrease in a parabolic manner to zero at the edge of the contact zone. Hence, the deformation at the center of the contact zone is given by

$$u_z = -\left[\delta - \frac{x^2}{2R}\right]$$

Equation 2-6

where δ is the maximum indentation and R is the equivalent radius.

The strain in the z direction is now expressed as

$$\varepsilon_z = \frac{\Delta t}{t} = -\frac{\left[\delta - \frac{x^2}{2R}\right]}{t}$$

Equation 2-7

where t is the nominal thickness of the rubber cover.

At the edge of the contact width, x =a and u_z = 0. Substitution of these values in Equation 2-6 yields Equation 2-8. Johnson uses Equation 2-8 to model the contact width. The radius (R) is calculated as equivalent radius of the form

$R = (R_1 \cdot R_2) / (R_1 + R_2)$, allowing it to be useful for two rollers in contact as well as a roller in contact with a plane.

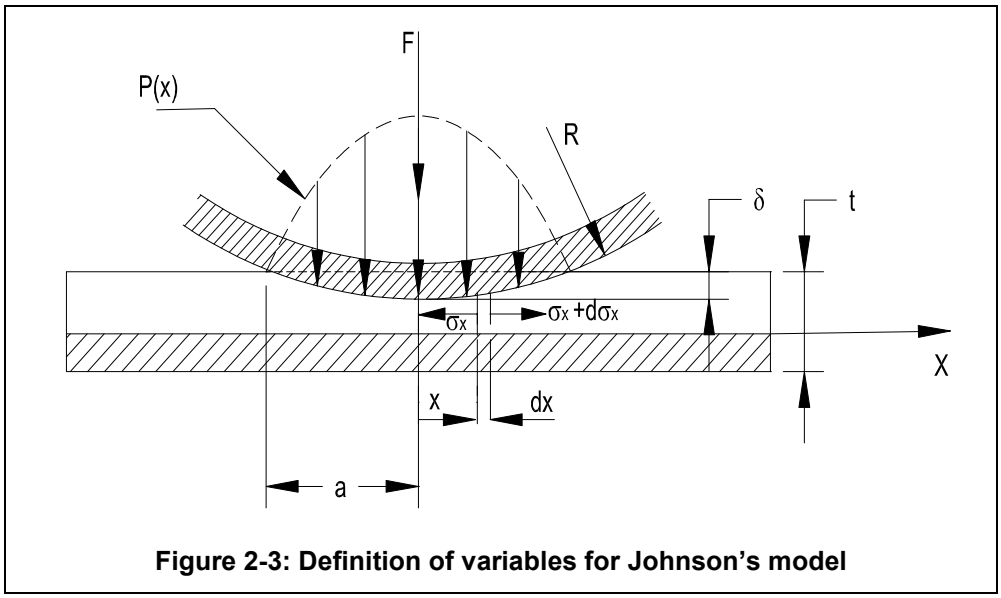

Figure 2-3: Definition of variables for Johnson's model

$$\delta = \frac{a^2}{2R}$$

Equation 2-8

Johnson assumes a bond between the elastic cover and the underlying roll and, hence, the strain in x direction is zero.

$$\varepsilon_x = \frac{1-\nu^2}{E_0}\sigma_x - \frac{\nu(1+\nu)}{E_0}\sigma_z = \frac{1-\nu^2}{E_0}\left[\sigma_x + \frac{\nu}{1-\nu}p(x)\right] = 0$$

Equation 2-9

If Equation 2-5 and Equation 2-7 are combined into a single equation and then with Equation 2-9, there are two equations and two unknowns. After eliminating σ_x, the pressure distribution p(x) is found as:

$$p(x) = \frac{(1-\nu)^2}{1-2\nu}\frac{E_0}{1-\nu^2}\frac{a^2}{2Rt}\left(1-\frac{x^2}{a^2}\right)$$

Equation 2-10

Integrating Equation 2-10 over the contact zone, the nip load per unit width (F) is expressed as a function of maximum penetration (δ) as:

$$F = \frac{4}{3}\frac{(1-\nu)^2}{1-2\nu}\frac{E_0}{1-\nu^2}\frac{\sqrt{2R}}{t}\delta^{3/2}$$

Equation 2-11

But, Johnson errs by a factor of 2 in his expression which was published as:

$$F = \frac{2}{3}\frac{(1-\nu)^2}{1-2\nu}\frac{E_0}{1-\nu^2}\frac{\sqrt{2R}}{t}\delta^{3/2}$$

Equation 2-12

Note that as ν approaches 0.5, F approaches infinity. While this makes sense for incompressible materials, it should be recognized that rubber is not truly incompressible.

2.2.2 Evan's Theory:

Evans [2] derived equations for modeling the contact of rubber covered rollers with that of a half plane, using Equation 2-8 to model the contact width. Evans then uses a different approach to derive his solution. He represents the average pressure in the contact zone as:

$$p_0 = \frac{F}{2\sqrt{2R\delta}}$$

Equation 2-13

Evans assumes that in the narrow zone of contact between the rubber covered roller and the plane, the elastic stresses are the same as if the whole surface of the roller were acted upon by an external uniform pressure given by Equation 2-13. This enabled him to obtain a relation between the average pressure and

the indentation, by means of Lame's solution for the elastic stresses in a hollow cylinder subjected to external and internal pressures.

The solution for the stresses at a radius r is:

$$\sigma_r = (A/r^2) + 2C$$

Equation 2-14

$$\sigma_\theta = -(A/r^2) + 2C$$

Equation 2-15

and

$$A = \frac{a^2 R^2 (p_0 - p_i)}{R^2 - a^2}$$

Equation 2-16

$$2C = \frac{p_i a^2 - p_0 R^2}{R^2 - a^2}$$

Equation 2-17

In an axisymmetric formulation, the general expression for tangential strain is:

$$\varepsilon_\theta = \frac{u}{r} = \frac{1}{E_0}\left[\left(\frac{-A}{r^2} + 2C\right) - \nu\left(\frac{A}{r^2} + 2C\right)\right]$$

Equation 2-18

Hence, the radial deformation u is:

$$u = \frac{1}{E_0}\left[\left(\frac{-(1+\nu)A}{r} + 2C(1-\nu)a\right)\right]$$

Equation 2-19

Evans assumes that the roller shaft restricts the radial deformation of the inside radius. Hence, the expression for u is equated to zero and substituting appropriate variables, the expression for pressures at the inner radius is derived as:

$$p_i = \frac{2p_0R^2}{a^2 + R^2 + \nu\left(R^2 - a^2\right)}$$

Equation 2-20

Substituting Equation 2-13 into Equation 2-20, and solving in terms of the nip load (F), yields:

$$F = \sqrt{\frac{2}{R}}\frac{2E_0\left[R^2(1+\nu) + a^2(1-\nu)\right]}{(R^2 - a^2)(1-\nu^2)}\delta^{3/2}$$

Equation 2-21

Note that F does not approach infinity when ν approaches 0.5 in this expression.

2.2.3 P.B.Lindley's Theory:

Lindley [10] performed experiments and derived expressions evaluating the non-linearity of rubber covered rollers. He developed a solution for a rubber covered roller in contact with a plane surface, which is equivalent to two identical rubber covered rollers in contact. Lindley assumed that a rubber covered roller under a compressive load contacts the surface through a long rectangular section with a width of 2a as shown in Figure 2-4.

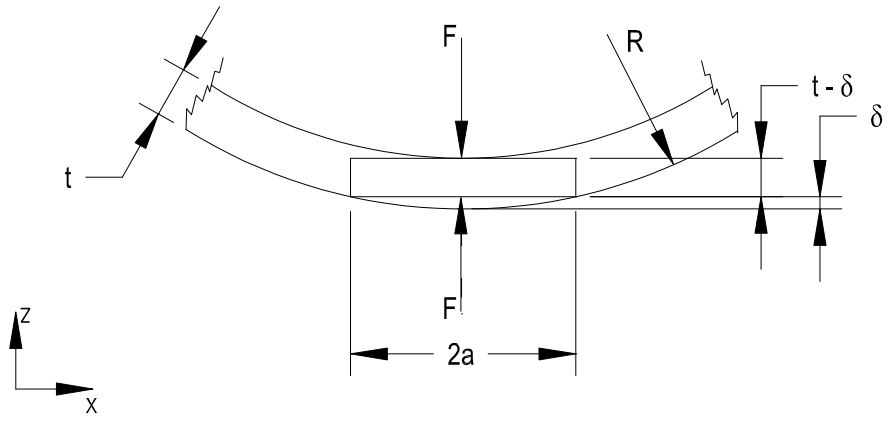

Figure 2-4: Definition of variables for Lindley's model

The area of contact, as compared to the width of roller, is small. Therefore, plane strain conditions are assumed to exist. It is also assumed that the incompressibility of the rubber cover does not impact the contact width. The contact width which Lindley developed is identical to Johnson's expression for contact width (Equation 2-8).

Lindley defines an incremental stiffness at any compressive deformation δ as:

$$\frac{dF}{d\delta} = \left[\frac{\text{modulus} \times \text{area}}{\text{thickness}} \right]_{\delta}$$

Equation 2-22

Under plane strain conditions, Lindley develops the compressive modulus including the confinement effect of rubber which is determined from:

$$E_{con} = \left[\frac{E_0 \left(1 + kS^2\right)}{1 - \nu^2} \right]_{\delta}$$

Equation 2-23

Where S is the shape factor defined as the ratio of the cross sectional area under load to the force free area. This factor accounts for the stiffening of rubber due to the confinement. For a rubber covered roller in contact with a half plane, the factor S is:

$$S = \left[\frac{\sqrt{2R\delta}}{t - \delta} \right]$$

Equation 2-24

k is an empirically derived factor based on the measured values of Young's modulus in the confined (E_{con}) and the unconfined state (E_0) and it makes the Equation 2-23 true. The values of k over a range of rubber hardness values are

tabulated by Lindley. (The value of 'k' ranges from 0.89 to 0.52 for the IRHD values ranging from 35 to 75). An expression for k is obtained by curve fitting these values and is used in the evaluations:

$$k = 0.00001 * (IRHD)^3 - 0.0016 * (IRHD)^2 + 0.0652 * (IRHD) + 0.1183$$

Equation 2-25

Based on these expressions and their appropriate substitution in Equation 2-22 and on integration of the resulting expression, Lindley developed a solution (Equation 2-26) for the relation between the force and penetration as:

$$F = E_o \sqrt{Dt} \left(\alpha_R + \frac{kD}{E_0} \beta_R \right)$$

Equation 2-26

where $\alpha_R = \frac{8}{3} \ln \left(\frac{1 + \sqrt{\frac{\delta}{t}}}{1 - \sqrt{\frac{\delta}{t}}} \right) - \frac{16}{3} \sqrt{\frac{\delta}{t}}$ and $\beta_R = \ln \left(\frac{1 + \sqrt{\frac{\delta}{t}}}{1 - \sqrt{\frac{\delta}{t}}} \right) - \frac{10}{3} \frac{\sqrt{\frac{\delta}{t}}}{1 - \frac{\delta}{t}} + \frac{4\sqrt{\frac{\delta}{t}}}{3\left(1 - \frac{\delta}{t}\right)^2}$

2.2.4 J.K.Good's Theory:

Good [4] developed an expression relating nip force to indentation similar to that of Johnson, which takes into account the rubber confinement similar to Lindley. The expression for pressure in the contact zone is:

$$p(x) = \left(1 + k \left(\frac{a^2}{t^2} \right) \right) \frac{E_c}{1 - \nu^2} \frac{a^2}{2Rt} \left(1 - \frac{x^2}{a^2} \right)$$

Equation 2-27

Integrating Equation 2-27 over the contact area, and substituting the expression for contact width by Equation 2-8, he expressed the relation between the load and indentation as:

$$F = \frac{4\sqrt{2}\, E_c \left[R\delta\right]^{\frac{3}{2}} \left(t^2 + 2\delta kR\right)}{3t^3\, R\left(1-\nu^2\right)}$$

Equation 2-28

The variable k used in the above expression is the same as developed by Lindley and R is the equivalent radius as expressed by Johnson. Good [4] used the expression given by Equation 2-3 (E_c) for Young's modulus of the rubber cover which is based on the hardness, strain rate and temperature, while the other authors use E_0 which is dependent on the hardness of the rubber given by Equation 2-1.

2.2.5 Parish's Theory:

Parish [12] analyzes the problem of a rubber covered roller in contact with a rigid roller based on the expressions developed by Hannah [7]. He has not derived a closed form relationship between the force and the indentation but such a relation can be derived from the empirical relationships he developed.

With one rigid and one homogeneous elastic roller in contact, the half nip width is given by:

$$a_0{}^2 = \frac{4FR\cdot\left(1-\nu^2\right)}{\pi E_0} \quad \text{and} \quad \frac{1}{R} = \frac{1}{R_1} + \frac{1}{R_2}$$

Equation 2-29

where R_1 and R_2 are the radii of the rollers.

Parish, also, expresses an empirical relationship between the two quantities $\frac{2R\delta}{t^2}$ vs. a_o/t. This relation is as shown in

Figure 2-5.

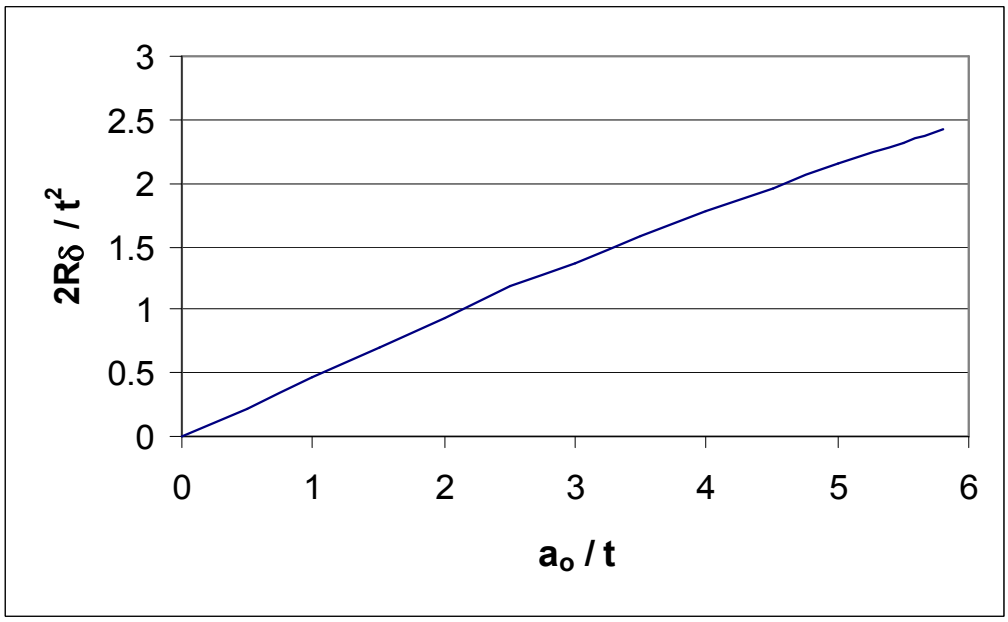

Figure 2-5: Variation of $\frac{2R\delta}{t^2}$ vs a_o/t

For a given value of F, the value of a_0 can be calculated from Equation 2-29. Then, from Figure 2-5, the quantity $\frac{2R\delta}{t^2}$ can be obtained and the indentation can therefore be derived from this expression:

$$\frac{2R\delta}{t^2} = -0.0152 \cdot \left(\frac{a_0}{t}\right)^2 + 0.5111 \cdot \left(\frac{a_0}{t}\right) - 0.0252 \qquad \text{where} \qquad \frac{a_0}{t} \neq 0$$

Equation 2-30

2.2.6 Miller's Theory:

Miller's [11] work on a theoretical relation between the applied force and cover indentation is based on Hannah [7] and Parish [14]. It includes the modifications related to the plane strain conditions, as opposed to the plane stress conditions considered by Hannah. He assumes that the rollers are

stationary, the frictional forces between them have a negligible effect on the indentation and the strains are arbitrary.

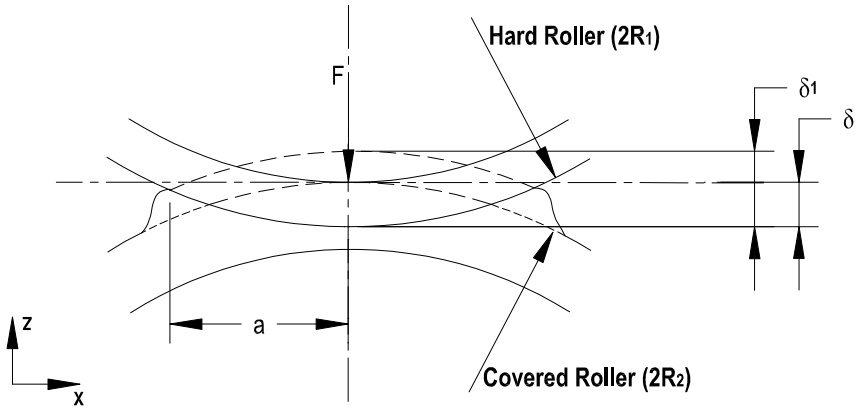

Figure 2-6: Definition of variables for Miller's derivation.

Miller assumes that the point at twice the contact width from the contact center is undisplaced. He derives an expression for the indentation as:

$$\delta = \frac{a^2}{2R}\left(1 + \delta_1(K,4)\right)$$

Equation 2-31

Where K is a variable and is equal to $\frac{a}{2t}$. Miller then derives the values for the quantity $\delta_1(K,4)$ with respect to K. (4 denotes the position of the undisplaced point on the cover boundary at twice the contact width from the contact center). He tabulates the variation of $\delta_1(K,4)$ with respect to K, which is shown in graphical form in Figure 2-7.

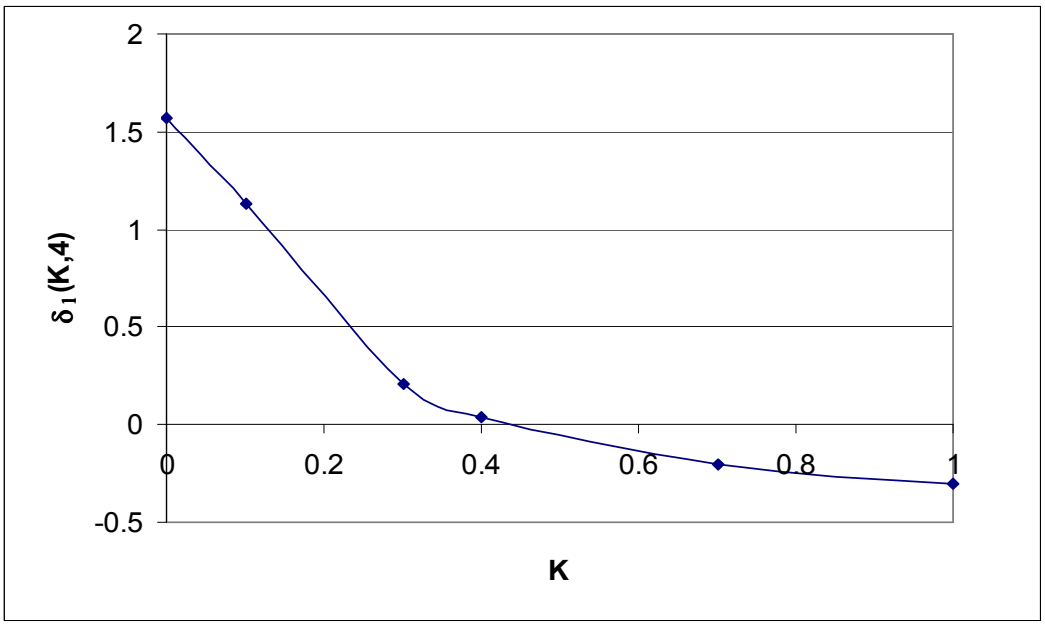

Figure 2-7: Variation of ($\delta_1(K,4)$) vs. K

The value of $\delta_1(K,4)$ is calculated based on the following expression obtained by curve fitting the above graph:

$$\delta_1(K,4) = -3.2765 \cdot K^3 + 7.9853 \cdot K^2 - 6.6255 \cdot K + 1.6224$$

Equation 2-32

From the results of Hannah, the relation between the load and nip width is given by Equation 2-29. The rubber cover indentations are calculated as follows.

1. For a given value of F, the value of 'a_0' is obtained using Equation 2-29.
2. The nip contact width 'a' is obtained using Equation 2-37 and Equation 2-38 as explained later in this chapter in section 2.3.1.
3. Using the contact width 'a', the value of K is determined. ($K = a/2t$).
4. From Figure 2-7, $\delta_1(K,4)$ can be computed for various values of K.
5. Using these values in Equation 2-31 indentations can be calculated for the given loads.

2.3 Tangential strain-Force/indentation relations:

The effect of the tangential strains, in the case of a rigid roller on a flexible plane, was observed and demonstrated by Osborne Reynolds in 1875 (as quoted in the publication “Slip in the rolling contact of two dissimilar elastic rollers”, by R.H. Bentall and K.L.Johnson in the International Journal of Mechanical Sciences in 1967). He deduced that the circumferential strains were tensile and explained his observations by the influence of Poisson’s ratio on the radial compressive strain, produced by the normal load. But, the Hertz contact theory states that the tangential strain, in general, is compressive and is zero for an incompressible material, like rubber. This anomaly is due to the fact that Reynolds used a thin rubber cover on a rigid hub. In these circumstances, the tangential strains are tensile. The velocity of the material element is also influenced by the state of strain in the deformed region.

The earliest work on the analysis of contact stresses was carried out by Hertz and his results have been quoted in by several authors in their studies. The contact stresses in the case of two rollers, one of which is assumed to be perfectly hard, with their axes parallel has been investigated by Thomas and Hoersch (as quoted in [7]). This work has also been widely quoted in many publications. An important work on the problem when the soft roller consists of a thin elastic cover on a hard supporting core has been published by Hannah [7].

Hannah’s work is for a plane stress case. The pressure distribution over the contact length is derived by Hannah as follows:

$$p(x) = \frac{2F}{\pi a_0}\left(1 - \frac{x^2}{a_0^{\,2}}\right)^{\frac{1}{2}} \quad for(-a_0 \le x \le a_0)$$

Equation 2-33

where F is the isolated force on the free face and $2a_0$ is the contact length.

The nip width in the contact zone is given by

$$a_0^{\,2} = \frac{4FR \cdot \left(1 - \nu^2\right)}{\pi E_0} \quad \text{and} \quad \frac{1}{R} = \frac{1}{R_1} + \frac{1}{R_2}$$

where R_1 and R_2 are the radii of the rollers in contact. These expressions have also been quoted and used in many publications.

The displacement due to the isolated force and the pressure distribution is determined. The stress function from the work of Coker and Filon (quoted by Hannah [7]) has been used with appropriate boundary conditions and the solution is obtained for a straight layer on a horizontal plane. Hannah's work states that the layer thickness is the most important factor determining the relation between loading and deformation of this type of roller.

2.3.1 Parish's Theory:

Parish G.J., [13] has derived the distribution of tangential strain due to contact pressure, at the surfaces in contact. His work has proved that in a system of metal and rubber covered rollers, the metal roller always has the higher apparent peripheral speed, whether it is driving or is driven by the rubber roller. This behavior is attributed to the extension of the rubber surface in the region of the nip, the extension is due in part to the contact pressure and in part to the presence of shear strains, consequent on the transmission of torque through the nip.

Parish has derived the tangential strains based on the work of Hannah [7], as mentioned above. His work gives the solution of the surface strain due only to

the contact pressure distribution and with the assumption that the rollers are stationary. A plane strain condition has been assumed and the appropriate modifications are made in the elastic constants. The notations used are the same as that of Hannah's.

For the case of a perfectly hard roller in contact with a homogenous elastic roller, the surface strains in the elastic roller, the roller axes being parallel is given by,

$$\varepsilon_{x_{y=0}} = (\frac{\partial u}{\partial x})_{y=0} = -\frac{2F}{\pi E_0 a}(1+\nu)(1-2\nu)(1-\frac{x^2}{a^2})^{0.5} \quad \text{for} \quad -a \le x \le a$$

Equation 2-34

The negative sign in the above equation indicates a compressive strain.

For the case of rollers with thin elastic cover, it is assumed that the cover is firmly bonded to its underlying shell and there is no normal or tangential displacement at the boundary. Based on the stress function given by Hannah, the surface strain is derived at the center of the contact zone and expressed in simple terms as:

$$(\frac{\partial u}{\partial x})_0 = \frac{2F(1-\nu)}{\pi E_0 a}(\psi(K,X))$$

Equation 2-35

Parish then evaluates the term $(\psi(K,X))$ and expresses its variation with respect to K for the maximum tangential strain. This relationship is expressed in graphical form as shown in Figure 2-8 . The polynomial derived by curve fitting this graph is expressed as:

$$\psi(K,0) = 0.3404 \cdot K^3 - 0.9506 \cdot K^2 + 0.8224 \cdot K - 0.0019$$

Equation 2-36

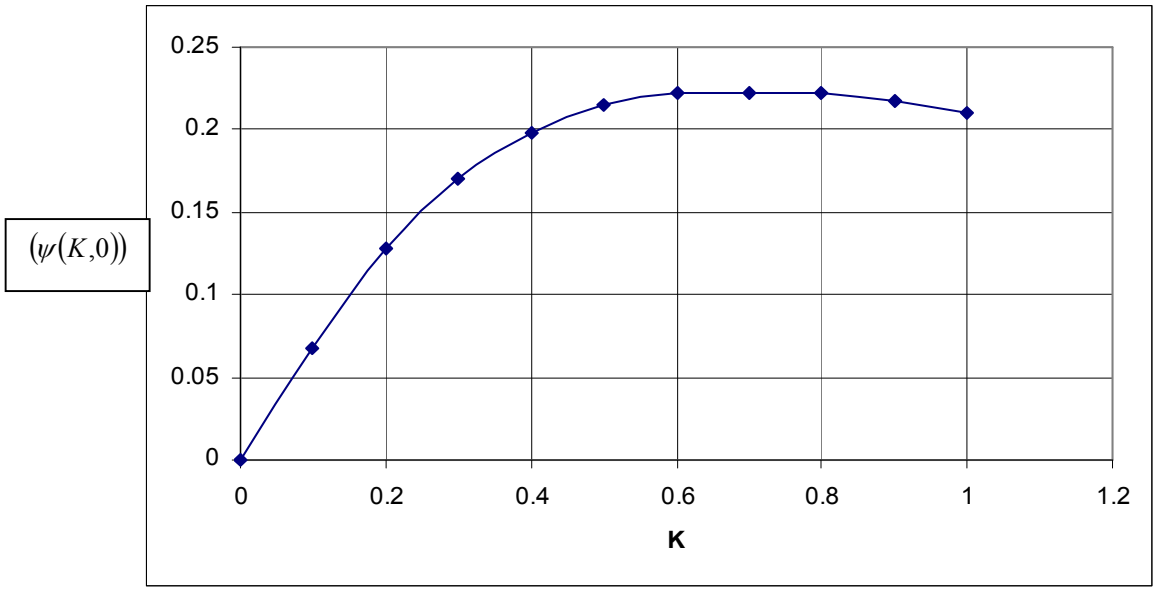

Figure 2-8: Variation of $(\psi(K,0))$ vs. K

The first step in the calculation of the tangential strain is the calculation of the nip contact width. This is done as explained hereunder.

Based on his experiments for a rubber covered roller in contact with a rigid roller, Parish expresses the relationship between the measured nip width (2a) and the nip width in case of a homogeneous elastic roller in contact with a rigid roller($2a_o$). This empirical relation is expressed in graphical form of variation of a/a_o vs. a_o/t.

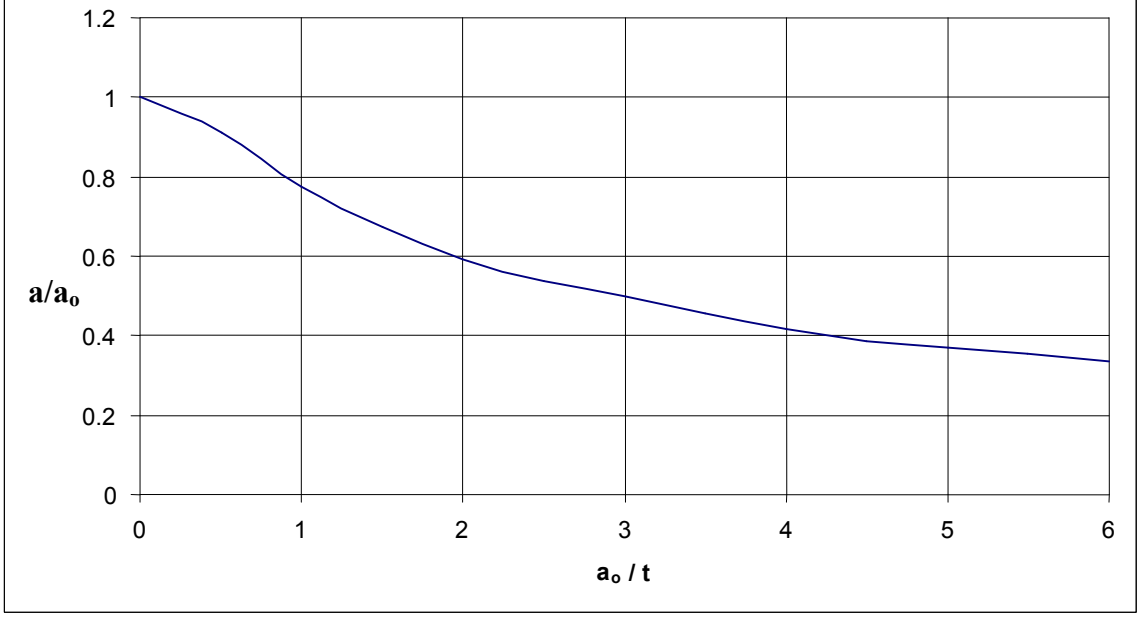

Figure 2-9: Variation of a / a_o vs. a_o / t.

For a given value of F, the value of a_0 can be calculated from Equation 2-29. The value of 'a' (the half contact width), can now be derived from the above graph. By applying numerical curve fitting techniques to this empirical graph, a polynomial expression can be derived. The value of a_o/t is less than two for the experimental data analyzed in this study. Hence, this part of the graph is curve fitted for better approximation.

$$\frac{a}{a_0} = 0.0458 \cdot \left(\frac{a_0}{t}\right)^3 - 0.1232 \cdot \left(\frac{a_0}{t}\right)^2 - 0.14 \cdot \left(\frac{a_0}{t}\right) + 1.0015 \qquad \text{where} \qquad \frac{a_0}{t} \le 2$$

Equation 2-37

And,

$$\frac{a}{a_0} = 0.0008 \cdot \left(\frac{a_0}{t}\right)^4 - 0.0124 \cdot \left(\frac{a_0}{t}\right)^3 + 0.0824 \cdot \left(\frac{a_0}{t}\right)^2 - 0.3274 \cdot \left(\frac{a_0}{t}\right) + 1.0037 \;\; ; \;\; \frac{a_0}{t} \ge 2$$

Equation 2-38

After determining the factor K from nip width (K= $\frac{a}{2t}$), the factor $(\psi(K, X))$ can be determined from the graph shown above. Then, using the Equation 2-35, the maximum tangential strain at the center of the contact width can be determined. The experimental results of Parish show that the distribution of the strain in the nip is dependent upon the parameter K. This parameter is the same as used in Miller's force vs. indentation relations, described earlier in this chapter.

2.3.2 Shelton's Theory:

Shelton [1] has derived an empirical equation that relates the percentage velocity change to the roller radius, radial deflection of the roller and the rubber thickness. The definition of variables for Shelton's equation is illustrated in Figure 2-10.

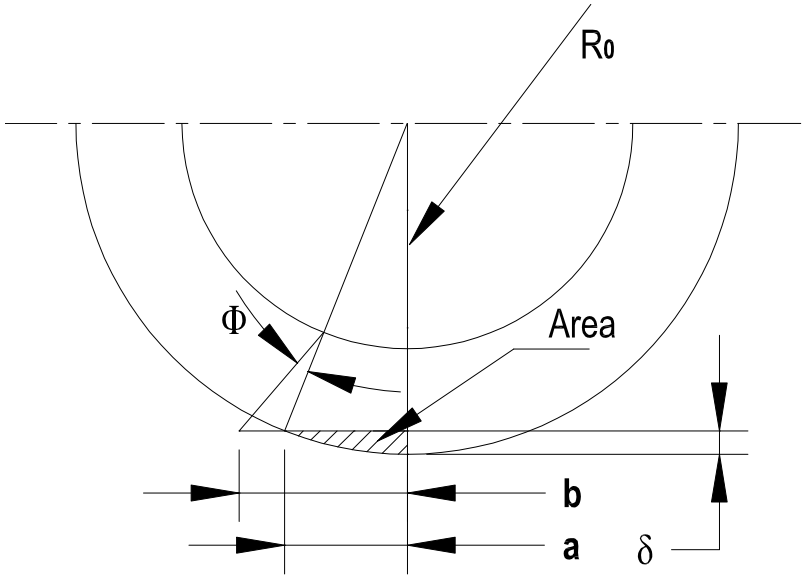

Figure 2-10: Definition of variables for Shelton's theory.

The angle Φ shown in the Figure 2-10 is determined from the triangle area displaced by the action of the nip:

$$\Phi = \frac{4\,\delta a}{3t^2}$$

Equation 2-39

Assuming that the velocity ratio is proportional to the angle Φ and adding a proportional constant, the following equation for change in velocity per unit velocity is derived.

$$\frac{\Delta V}{V} = \frac{0.25\,\delta a}{t^2}$$

Equation 2-40

Substituting for small deflections, the equation for the velocity change is expressed as:

$$\frac{\Delta V}{V} = \varepsilon = \frac{0.35\,R^{\frac{1}{2}}\delta^{\frac{3}{2}}}{t^2}$$

Equation 2-41

This equation gives the increment in strain in the web due to the speed increase of the rubber cover in the contact zone.

2.3.4 Good's Theory:

Good [3] derived a simple approximation for the tangential strains in the rubber cover as a result of the rubber compression. His assumptions are based on the studies conducted by Johnson and Lindley. Their models assume that the nip load is reacted by a block of rubber with a width equal to that of the contact zone. From this assumption, the circumferential strains can be related to the radial strains by the following expression:

$$\varepsilon_\theta = -\nu\varepsilon_r$$

Equation 2-42

The radial strains are maximum at the center of the contact zone and decreases to zero at the ends of the zone. Hence, the simple average is :

$$\varepsilon_r = -\frac{\delta}{2t}$$

Equation 2-43

Now, as Poisson's ratio approaches 0.5 for rubber, Equation 2-43 yields the following expression for the average tangential strain:

$$\varepsilon_\theta \approx \frac{\delta}{4t}$$

Equation 2-44

2.4 Lateral deformation-tangential strain relation:

Shelton [15] formulated an expression which relates the tangential strain to lateral deformation of the web. The term 'entering web span' is the length of the web from the center of the nip to the center of the roller prior to the nip. Shelton developed a second order differential equation for an entering span:

$$\frac{d^2y}{dx^2} = -\frac{12M}{KK_{sweb}W^3}$$

Equation 2-45

The boundary conditions are illustrated in Figure 2-11.

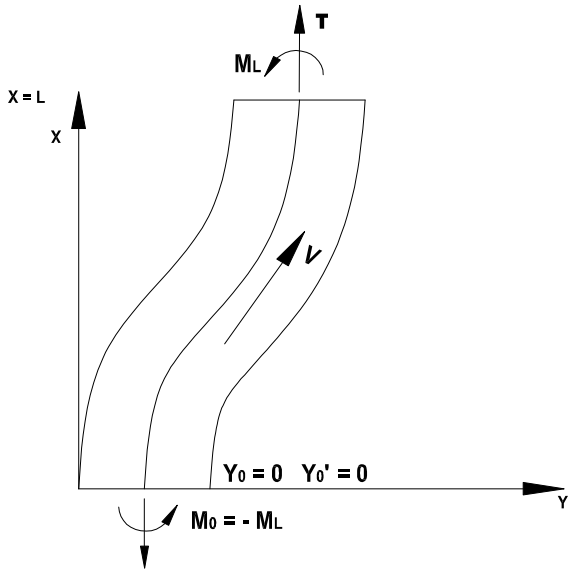

Figure 2-11: Boundary conditions of the web deflected in the nip

The moments calculated at any point along the web span is given by:

$$M = -M_L + \frac{2M_L + Ty_L}{L}x - Ty$$

Equation 2-46

$$KK_{web} = \frac{\sqrt{\frac{12T}{KK_{sweb}W}}}{W}$$

Equation 2-47

Using Equation 2-46 and Equation 2-47 in Equation 2-45, and applying the boundary conditions and upon integration, the following solution is obtained:

$$Y = \frac{M_L}{T}\left[\left(\cosh KK_{web}x - 1\right) - \frac{\sinh KK_{web}L}{\cosh KK_{web}L - 1}\left(\sinh KK_{web}x - KK_{web}x\right)\right]$$

Equation 2-48

Since it is easier to use the differential strain as the input rather than the moment, the moments are related to the differential tension in the web as follows:

$$M_L = \frac{W}{12}\Delta T$$

Equation 2-49

And the specific stiffness is:

$$KK_{sweb} = \frac{\frac{\Delta T}{W}}{\Delta \varepsilon}$$

Equation 2-50

Rearranging Equation 2-49 and Equation 2-50, and using Equation 2-47 in the resulting expression, an equation that relates the moment to the change in strain is obtained:

$$\frac{M_L}{T} = \frac{\Delta \varepsilon}{KK_{web}{}^2 W}$$

Equation 2-51

Substituting this equation into Equation 2-48, the equation for lateral deflection, which relates to the differential strain, is derived:

$$Y = \frac{\Delta \varepsilon}{KK_{web}{}^2 W}\left[\left(\cosh KK_{web}x - 1\right) - \frac{\sinh KK_{web}L}{\cosh KK_{web}L - 1}\left(\sinh KK_{web}x - KK_{web}x\right)\right]$$

Equation 2-52

The study of the lateral steering of a web in a differentially loaded nip of rubber covered rollers requires the determination of the lateral web deflection. As an input to the determination of the deflection, the differential strains in the nip have to be computed. Hence, algorithms which relate force vs. indentation and strains to force / indentations become indispensable.

The present investigation will attempt to verify all the force–indentation relationships described earlier, quantify the degree of closeness to the experimental data and analyze which of these close formed relations best predict the nip behavior. The force-indentation algorithm chosen will be used as an input for the tangential strain and force / indentation relationships. A similar analysis will be carried out for the best force or indentation-tangential strain algorithm. The algorithm chosen will be used to compute the strains and hence compute the lateral deflection. The variation of this theoretical prediction of the web deflection with respect to the experimental data, if any, will be explored.

CHAPTER 3

Force vs. Indentation Algorithms

Good [5] conducted experiments to measure the deformations in the rubber cover with respect to the nip load for different sets of roller pairs. A test program was set up such that the deformations of the nip roller pairs could be monitored in a web line as the nip load was varied. The deformations were monitored using linear variable differential transformers. Nip loads were applied using pneumatic cylinders that were controlled with regulators. A simple schematic of the set up is as shown in the Figure 3-1.

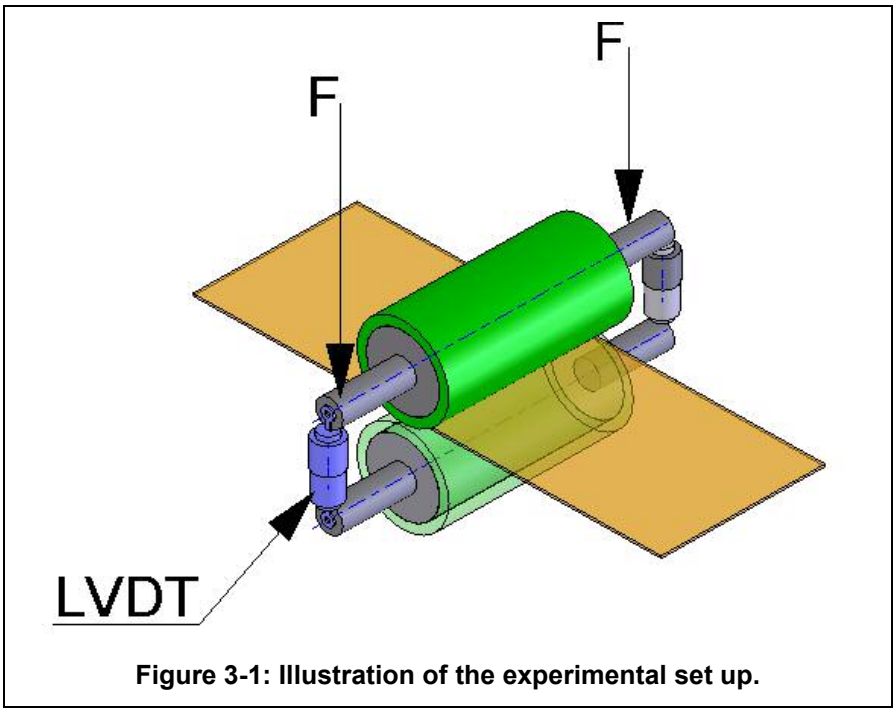

Figure 3-1: Illustration of the experimental set up.

These experiments were conducted for the cases where two identical rubber covered rollers were in contact and for the cases where a rubber covered roller was in contact with a metal roller, for different set of roller pairs. Each of these cases will be referred to as a 'roller test case'. The experiments for load vs. indentation comprised 10 different roller test case situations which are listed in Table 3-1. The experiment was conducted at a web velocity of 100 fpm. The material used was a polyester web with a width of 12 inches and a thickness of 0.00092 inches.

Case	Roller A			Roller B		
	OD (in.)	CT (in.)	HARDNESS (Shore A)	OD (in.)	CT (in.)	HARDNESS (Shore A)
1	3.5	0.75	40	2.9	---	RIGID
2	3.5	0.75	40	3.5	0.75	40
3	2.5	0.25	80	2.9	---	RIGID
4	2.5	0.25	80	2.5	0.25	80
5	5.0	0.50	60	2.9	---	RIGID
6	5.0	0.50	60	5.0	0.50	60
7	7.5	0.75	80	2.9	---	RIGID
8	7.5	0.75	80	7.5	0.75	80
9	6.5	0.25	60	2.9	---	RIGID
10	6.5	0.25	60	6.5	0.25	60
OD ---- Outer Diameter of the Roller						
CT ---- Rubber Cover Thickness						

Table 3-1: Roller Test Cases

The deformations in the rubber cover were measured at 10 different load levels for each set of rollers, starting at 0.5 pli and proceeding to 10 pli in 0.5 pli increments.

Force-indentation relationships developed by Johnson, Evans, Lindley, Good, Parish and Miller were described in CHAPTER 2. The objective, now, is to

determine which closed form relationship is the best for this load range and the rollers presented in Table 3-1, by comparing them with the experimental deformation data available.

The theoretical results of all the algorithms are obtained by applying them to the different load levels and roller cases. The Poisson's ratio used in all these calculations is 0.46.

3.1 Application of Johnson's theory:

Hergenrether [8] compared Johnson's Equation 2-11and Equation 2-12 in his thesis. He showed that Johnson's Equation 2-12, which is in error, as shown in CHAPTER 2, yields results closer to the experimental data than Equation 2-11. Based on Hergenrether's results, Johnson's Equation 2-12 is chosen in this study for further analysis.

Johnson's expression includes the Young's modulus of the rubber as a constant value E_o, depending only on the hardness of the rubber. This value is given by Equation 2-1.

This expression is modified by the compression modulus developed by Good, given by Equation 2-3. Johnson's modified expression is now stated as:

$$F = \frac{2}{3}\frac{(1-\nu)^2}{1-2\nu}\frac{E_c}{1-\nu^2}\frac{\sqrt{2R}}{t}\delta^{3/2}$$

Equation 3-1

Johnson's unmodified expression given by Equation 2-12 and the modified expression given by Equation 3-1 will be compared with the experimental data. They will be denoted as 'KLJ' and 'KLJMod' respectively.

3.2 Application of Lindley's theory:

Lindley's expression for the load vs. deformation relationship is given by Equation 2-26. The Young's modulus in this equation is replaced by the Equation 2-3. The resulting equation is expressed as:

$$F = E_c\sqrt{Dt}\left(\alpha_R + \frac{kD}{E_0}\beta_R\right)$$

Equation 3-2

Where $\alpha_R = \frac{8}{3}\ln\left(\frac{1+\sqrt{\frac{\delta}{t}}}{1-\sqrt{\frac{\delta}{t}}}\right) - \frac{16}{3}\sqrt{\frac{\delta}{t}}$ and $\beta_R = \ln\left(\frac{1+\sqrt{\frac{\delta}{t}}}{1-\sqrt{\frac{\delta}{t}}}\right) - \frac{10}{3}\frac{\sqrt{\frac{\delta}{t}}}{1-\frac{\delta}{t}} + \frac{4\sqrt{\frac{\delta}{t}}}{3\left(1-\frac{\delta}{t}\right)^2}$

Lindley's unmodified expression given by Equation 2-26 and the modified expression given by Equation 3-2, will be compared with the experimental data. They will be denoted as 'Lindley' and 'Lindleymod' respectively.

3.3 Application of Evan's theory:

Evan's expression for the load vs. deformation relationship is given by Equation 2-21. A similar modification is done to this expression by replacing the Young's modulus by Equation 2-3. The resulting equation is expressed as:

$$F = \sqrt{\frac{2}{R}}\frac{2E_c\left[R^2(1+\nu)+a^2(1-\nu)\right]}{(R^2-a^2)(1-\nu^2)}\delta^{3/2}$$

Equation 3-3

Evan's unmodified expression given by Equation 2-21 is denoted as 'Evans' and the modified expression given by Equation 3-3 is denoted as 'Evansmod'.

3.4 Application of Good, Parish and Miller's theories:

Modifications are done for the Young's modulus by Equation 2-3 in Parish's empirical algorithm and also in Miller's algorithm. They are referred to as 'Parishmod' and 'Millermod' respectively in the analysis.

Good's expression for force-indentation relationship used his modified expression for Young's modulus. Hence there is no modification done in his equation. His algorithm will be referred to as 'Good' in the analysis.

3.5 Comparison of Models:

The comparison of the load-indentation relationship predicted by all these algorithms, with the experimental data is shown for a roller test case 6 in Figure 3-2, as a sample.

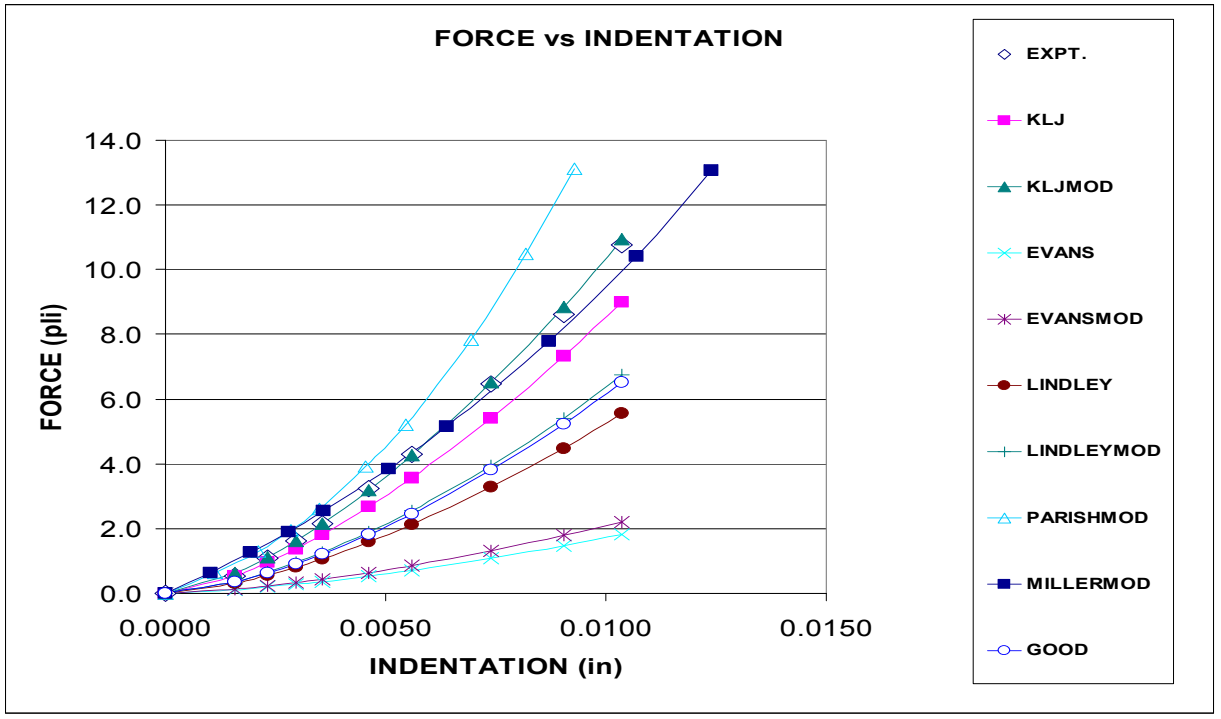

Figure 3-2: Comparison of the theoretical and the experimental values for roller case 6.

Comparisons of the theoretical results with the experimental data for all the individual roller cases are listed in Appendix A.

After the theoretical calculations are done, the analysis is done for each roller case individually. The experimental values and the corresponding theoretical values calculated using each algorithm for all the load levels are analyzed. The variation of the theoretical prediction to that of the experimental data for each load level is quantified by computing the ratio of the theoretical value to that of the experimental value. Then, for each theory, an average of these ratios for all the load levels is obtained. This average ratio helps in determining how well a theory predicts the experimental data for a particular roller case. The prediction of the theory is better when its average ratio is closer to 1. Hence, an algorithm whose average ratio shows a minimum variation to 1 is the best for the roller case analyzed.

The analysis for roller case 6 is shown as sample in Table 3-2. The ratios for each load level and the average ratio for all the load levels is listed for each theory.

For this particular roller case, the modified algorithm of Johnson proves to be the best with an average ratio of 1.025. Miller's modified algorithm is the second best.

Force vs. Indentation									
Load	**Miller mod**	**Parish mod**	**KLJ**	**KLJmod**	**Evans**	**Evans mod**	**Lindley**	**Lindley mod**	**Good**
0.5	0.646	0.713	0.990	1.1501	0.198	0.23	0.577	0.67	0.64
1	0.835	0.907	0.885	1.0379	0.177	0.208	0.518	0.608	0.581
1.5	0.943	0.965	0.851	1.0041	0.17	0.201	0.5	0.59	0.565
2	1.008	0.979	0.843	0.9982	0.169	0.2	0.497	0.589	0.565
3	1.096	0.985	0.830	0.9886	0.166	0.198	0.493	0.587	0.564
4	1.144	0.973	0.828	0.9912	0.166	0.199	0.495	0.593	0.57
6	1.180	0.938	0.838	1.0102	0.169	0.203	0.507	0.611	0.59
8	1.183	0.907	0.849	1.0281	0.171	0.207	0.519	0.628	0.608
10	1.194	0.896	0.836	1.0149	0.169	0.205	0.515	0.626	0.607
Avg. ratio	1.0255	0.918	0.861	1.0248	0.173	0.206	0.513	0.611	0.588
Var.	0.0255	0.082	0.139	0.0248	0.827	0.794	0.487	0.389	0.412
Minimum variation :			**0.0248**				**KLJMOD**		

Table 3-2: Comparison of the ratios of the theoretical to experimental values for roller case 6.

The analysis explained so far helps in predicting the best algorithm for a particular roller test case. As mentioned earlier, the experiments were conducted for 10 different roller test cases. It follows that the data for all the roller test cases should be analyzed, to determine the algorithm which gives the overall best results.

The average ratios for each algorithm are calculated earlier for individual roller cases. An average of all these average ratios for different roller cases is then calculated for every theory. This is called the Overall Average Ratio. The Overall Average Ratio (OAR) hence indicates how closer the theoretical results are to the experimental data. Similar to earlier explanations, it can now be stated that the results of an algorithm is better as its Overall Average Ratio is closer to 1. The overall analysis is shown in Table 3-3.

Overall Comparison of Average ratios									
Roller cases	**Miller mod**	**Parish mod**	**KLJ**	**KLJmod**	**Evans**	**Evans mod**	**Lindley**	**Lindley mod**	**Good**
1	1.613	1.557	0.347	0.449	0.345	0.448	0.206	0.268	0.255
2	1.608	1.488	0.426	0.541	0.186	0.236	0.257	0.327	0.315
3	0.714	0.691	1.011	1.187	0.415	0.49	0.658	0.777	0.73
4	0.803	0.752	1.132	1.312	0.227	0.263	0.665	0.77	0.734
5	0.764	0.737	1.021	0.744	0.569	0.701	0.604	0.744	0.708
6	1.025	0.918	0.861	1.025	0.173	0.206	0.513	0.611	0.588
7	0.410	0.678	1.061	1.195	0.815	0.918	0.752	0.847	0.794
8	0.570	0.553	1.208	1.310	0.251	0.273	0.735	0.797	0.757
9	0.906	0.795	1.111	1.397	0.281	0.354	0.686	0.863	0.833
10	1.200	0.009	0.619	0.750	0.05	0.060	0.414	0.502	0.499
OAR	0.9616	0.818	0.88	0.991	0.331	0.395	0.549	0.651	0.621
Var.	0.038	0.182	0.12	0.009	0.669	0.605	0.451	0.349	0.379
Min. variation (overall) :				**0.009**			**KLJMOD**		

Table 3-3: Overall Comparison of the ratios of the theoretical to experimental values.

3.6 Summary:

When the whole data range of all the load levels and the roller cases were analyzed, Johnson's modified Algorithm showed minimum variation of 0.009 from the experimental data. Hence, Johnson's modified algorithm will be used as an input for the analysis of the tangential strain vs. force / indentation relationships discussed in CHAPTER 4. Parish's algorithm is based on empirical data. In Miller's algorithm, calculation of the nip contact width is based on empirical data. Evans assumes uniform external pressure acting on the surface of an incompressible roller. Yet he uses Lame's solution for the elastic stresses in the development of his algorithm. Some confusion exists in his assumptions. It should be noted that Johnson's algorithm which was selected to be the "best" is "best "only for the rollers and load ranges used in these experiments. At higher load levels, the confinement of the rubber which is addressed by Lindley's and Good's models becomes important. Thus the "best" algorithm would have not been Johnson's, had a larger range of load been allowed in the experiments.

CHAPTER 4

Tangential strain vs. Force/Indentation Algorithms

After determining the best closed form algorithm available for the force vs. indentation relationships, an algorithm that relates the tangential strains in the rubber cover to the nip force or indentation has to be determined.

Parish [13] derived an expression (Equation 2-35) that relates the maximum tangential surface strain to the force applied. His derivation followed the work of Hannah [7]. Shelton [1] derived an expression which gives the increment in strain in the web due to the speed increase of the rubber cover in the contact zone. His expression (Equation 2-41) is an empirical relation that determines the change in velocity per unit velocity which can be related to the tangential strain. Good [3] derived a simple expression which determines the average tangential strain in the rubber cover in the contact zone. These three algorithms were explained in detail in CHAPTER 2. This chapter includes the details about the experiments conducted and the procedures involved in determining the algorithm whose results best fit in the experimental data.

Good [3] conducted experiments to measure the variations in the length of the web traversed ($\frac{\Delta L}{L}$) and compared the experimental data with the expression

he developed for the average tangential strains. His experimental set up is explained in Figure 4-1.

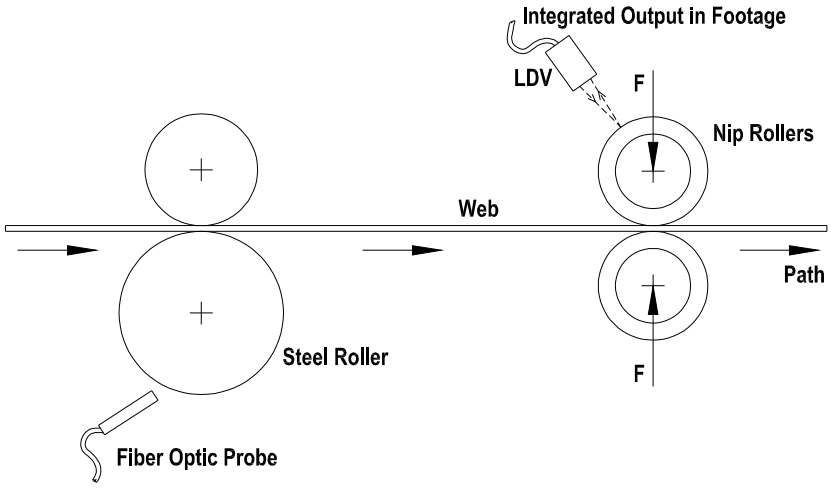

Figure 4-1: Experimental set up for strain measurement.

When the target passed the fiber optic probe at the upstream roller, the output signal from the probe triggered and rolled the Laser Doppler Velocimeter (LDV). The web drove the rubber covered rollers and the output of the LDV was a measure of the distance the undeformed rubber cover surface had moved tangentially. After three revolutions of the upstream roller, the output of the fiber optic probe was used to stop and hold the integrated output of the LDV. The amount of web which transited the upstream roller was $3\pi D$ during this period. Since the back (undeformed) side of the rubber covered roller was traveling at a lower velocity than the web, the length of the undeformed surface of the rubber cover which passed during the same time period was less than that of the length of the web which passed the upstream roller.

This experiment was conducted for the same sets of roller cases and the same sets of load levels for which the force vs. indentation experiments were carried out. The details of these roller cases and the load levels have already been described in CHAPTER 3.

The length of the web traversed on the rubber covered roller for 3 revolutions of the steel roller on Input drive was measured. Ten data points were collected at every load level and the average and standard deviation of these data were calculated. The average value of these 10 data points was then used for further calculations for that particular load level. Measurements were taken for 10 load levels for each roller case.

The experiment is repeated for all the 10 roller cases. The ratio of the change in the length of the web traversed to that of the original length is calculated as follows:

$$\frac{\Delta L}{L} = \frac{\pi D_1 - \frac{L}{3}}{\pi D_1} = \frac{\Delta V}{V}$$

Equation 4-1

where D_1 denotes the calculated diameter of the steel roller and L is the length of the web traversed on the rubber covered roller for 3 revolutions of the steel roller in inches.

The same value is also determined by using the measured value of the steel roller diameter. This is expressed by Equation 4-2 in which D_2 denotes the measured diameter of the steel roller.

$$\frac{\Delta L}{L} = \frac{\pi D_2 - \frac{L}{3}}{\pi D_2} = \frac{\Delta V}{V}$$

Equation 4-2

There was variation between the data obtained using Equation 4-1 and Equation 4-2. Hence, a confidence interval at 90%, which statistically states the estimated range in which these experimental data would fall, was calculated for the measured data points. The variation between the data obtained by Equation 4-1and Equation 4-2 along with the confidence level calculated for the measured data is plotted in Figure 4-2 for roller case 1.

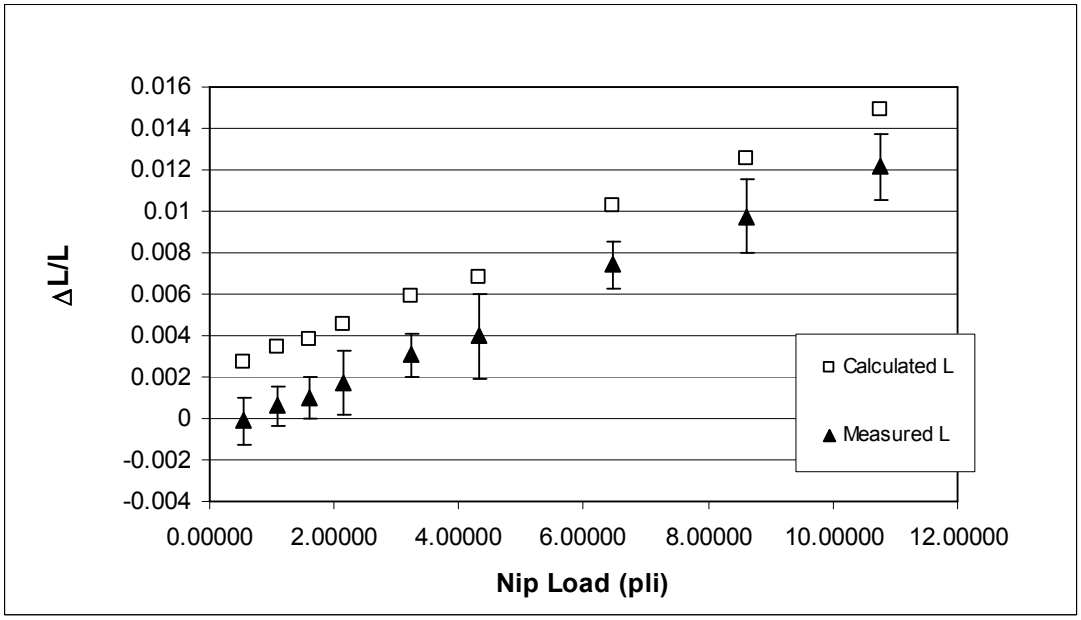

Figure 4-2: Comparison of the measured and calculated length variations vs. load for roller case 1

The fluctuation in the data at very low load levels is clearly visible for certain roller cases. To illustrate this, a graph similar to Figure 4-2 is plotted in Figure 4-3 for roller case 8. The resolution of the experimental method might be the

probable cause for this anomaly. To extract meaningful information from the data obtained, Good statistically adjusted the data by making corrections for the zero level. The experimental data obtained for the lowest load level of 0.5pli was set as the standard zero and all the other data points were adjusted accordingly. A constant value of 0.001 was added to all the data points obtained since the minimum resolution of the method was assessed at 0.001.

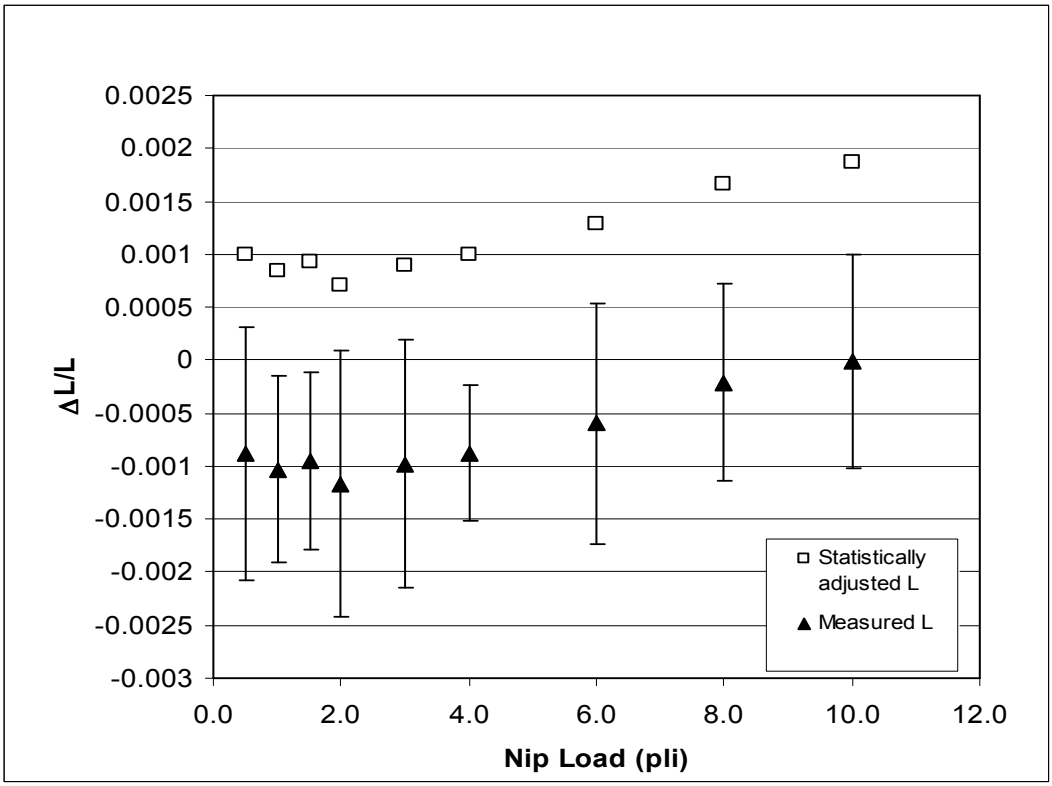

Figure 4-3: Comparison of the measured and calculated length variations vs. load for roller case 8

This statistically adjusted data was used for comparison with all the theories.

4.1 Application of Parish's theory:

Parish derived an expression which relates the maximum tangential surface strain in the rubber cover to the applied nip load (Equation 2-35). The

Young's modulus used in Parish's expression is replaced by the empirical relation for compression modulus developed by Good (Equation 2-3). This new expression is used to compute the maximum tangential strains and is compared with the adjusted experimental data.

4.2 Application of Shelton's and Good's theories:

Shelton's empirical expression relates the percentage velocity change to the roller radius, cover thickness and the radial indentation. Good's expression also relates the average tangential strain to the rubber cover thickness and the indentation. The indentation measured earlier for the same load levels and roller cases, as explained in CHAPTER 3 are used as an input to these theories.

A comparison of the theoretical calculations using the three algorithms to that of the experimental data is shown in Figure 4-4 for roller test case 6. Similar comparisons for all the other roller test cases are listed in APPENDIX B.

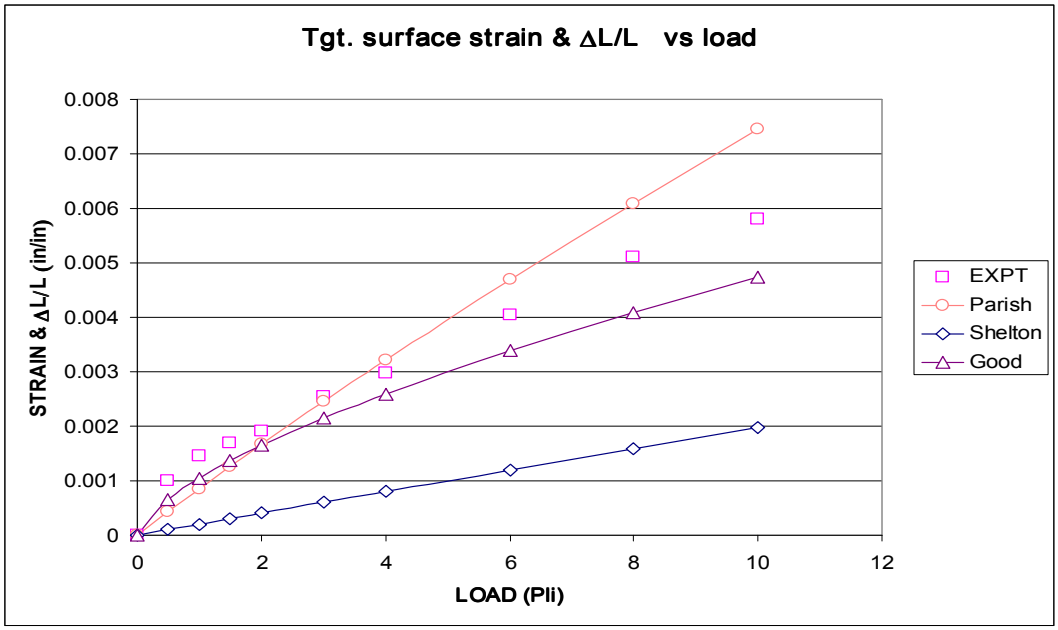

Figure 4-4: Comparison of the theoretical and experimental strains vs. Nip load for roller case 6

The theoretical values for the tangential surface strain of the rubber cover in the contact zone are computed for all the load levels and roller cases.

4.3 Analysis:

After computing all the theoretical values using the three closed form algorithms available, an analysis similar to the one done for the force vs. indentations is carried out.

As explained earlier, the analysis is first carried out for the Individual roller cases for various load levels. A ratio of the theoretical value to that of the experimental data is computed for each load level. A sample calculation for roller case 6 is shown in Table 4-1. A theory is closer to the experimental data if its average ratio is closer to 1 for the particular roller case.

Strains vs. Force/Indentation			
Load	**Parish**	**Shelton**	**Good**
0.5	0.775	0.189	0.744
1	1.322	0.331	1.040
1.5	1.569	0.402	1.106
2	1.608	0.4212	1.054
3	1.502	0.408	0.894
4	1.593	0.447	0.891
6	1.610	0.475	0.829
8	1.669	0.513	0.815
10	1.687	0.537	0.793
Average ratio	1.482	0.414	0.907
Variation	0.482	0.586	0.093
Min.Variation (Best Fit):		**0.093**	**GOOD**

Table 4-1: Comparison of the ratios of the theoretical to experimental strains for roller case 6.

For roller case 6, the average ratio for Good's theory was very close to 1 compared to the other theories. Hence, Good's theory is the best for this case.

The average ratios thus computed for each roller case are then used to calculate the Overall Average Ratio (OAR) for all the load levels and roller cases. The overall Average ratio is also computed in the same procedure as explained in CHAPTER 3. The OAR calculation for roller case 6 is shown in Table 4-2.

	Average Ratios		
Roller cases	**Parish**	**Shelton**	**Good**
1	1.697	0.426	1.503
2	1.311	0.320	1.452
3	0.887	0.219	0.873
4	1.060	0.269	0.872
5	0.985	0.239	1.183
6	0.924	0.232	0.802
7	1.406	0.356	1.177
8	1.482	0.414	0.907
9	0.632	0.153	0.793
10	0.455	0.112	0.845
OAR	1.084	0.274	1.041
Variation	0.084	0.726	0.041
Minimum Variation:		**0.041**	**GOOD**

Table 4-2: Computation of the Overall average Ratio

The Overall average ratio for Good's theory is 1.041 and it is the closest to the experimental data when compared with Parish's and Shelton's theories. Hence, Good's theory best predicts the relationship between the tangential strain and the indentation of the rubber cover. Parish's theory is second best. Good's theory will be used for further calculations in determining the lateral deflections, explained in CHAPTER 5.

CHAPTER 5

LATERAL WEB STEERING

When the nip is loaded differentially, the load varies across width of the web transiting the nip in the Cross Machine Direction (CMD). The indentations caused in the rubber cover vary along the width too. This variation, in turn, causes the tangential strains to vary across the CMD. As described in CHAPTER 4, the expression developed by Good [3] to describe the relationship between the indentations and the tangential strains is the best among the available closed form relationships. The varying tangential strains in a differentially loaded nip can be predicted by Good's algorithm and can be used to calculate the lateral deformation of the web as it passes through the nip of rubber covered rollers.

The tangential strains predicted by Good for the varying indentations in the rubber cover along the roller length will be used as an input for computing the lateral deflection of the web. Good [5] developed a finite element code to predict the force/deformation expressions in the nip contact width of a metal roller with a rubber covered roller (MRNIP) as well as in the nip contact width of two identical rubber covered rollers in contact (RRNIP). These codes use finite beam elements to model the core of the rollers and the Winkler foundation models for the rubber cover. They help to estimate the effective load acting at various

points across the roller length. Good's algorithm for the tangential strains will be incorporated in the RRNIP. Thus the strains will be calculated at various points across the roller length and the average tangential strain can be calculated. This average strain will be used in Shelton's [15] closed form expression (Equation 2-52) to compute the lateral deflection of the web. The lateral deflection can be computed at various points along the web length. Ahmad [1] conducted experiments to measure the maximum lateral deflection of a web in a differentially loaded nip. The theoretical results computed using Shelton's [15] equation will be compared with Ahmad's experimental data.

This chapter gives a brief description of Shelton's expression for computing the lateral web deflection, the experimental set up used by Ahmad and the NIPCODES MRNIP and RRNIP developed by Good. This chapter also describes how the NIPCODES are used to calculate the lateral web deflection and compares the theoretical results with that of the experimental web deflection data.

5.1 Lateral deflection Algorithm:

Shelton [15] developed an expression (Equation 2-52) for the lateral deformation of the web as it transits, as a function of the differential strain across the web width. This was done because in a practical situation, the determination of the differential strain would be easier than the determination of moments. The variables used in Shelton's [15] expression have been described in CHAPTER 2. His expression enables the computation of the lateral deflection of the web at various positions along its length.

The differential strain across the web width, a dimensionless expression KK_{web} (Equation 2-47)which is computed using the total tension in the web and the web stiffness, and the position along the length of the web at which the deflection needs to be computed are required as inputs to Shelton's [15] expression. The computation of these terms will be explained later in this chapter.

5. 2 Experiment for Lateral deflection:

Ahmad [1] conducted experiments to monitor the web deflections as it transits the nip. A nip set up that could be used for uneven load application was used in his experiments. The nip set up was installed on a web line that allowed continuous transport of the web. Uneven load application was made possible by applying loads on both sides of the nip independently. The web was guided at the entry side using an edge guiding mechanism. A schematic of his experimental set up is as shown in Figure 5-1.

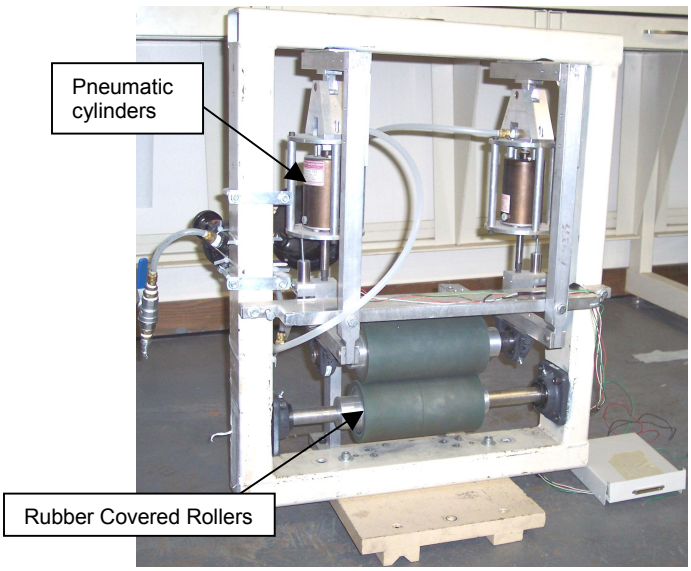

Figure 5-1: Ahmad's experimental nip set up for uneven loading.

The maximum lateral deflection of the web occurs at the nip and the web remains in the maximum deflected state until it reaches the edge guiding mechanism. The guiding mechanism helps to position the web to its non-deflected state at its entry to the nip.

Ahmad used identical rubber covered rollers in his experiments. The rollers were made with a metal core and a rubber cover. The outer diameter of each of these rollers was three inches. The rubber covers were half inch in thickness. Nitrile rubber was used for the covers. Three sets of such rollers were used which had rubber covers with different hardness values. A polyester web was used in these experiments. The web was 6 inches wide and 0.002 inches thick. The elastic modulus of the web material is 600,000 psi.

The dimensional details and of the rubber rollers and the web are described in Table 5-1. The material properties of the rubber cover and the web are also given.

Case	**Rollers**			**Web**
Case	OD (in.)	CT (in.)	HARDNESS (SHORE A)	ENTRY SPAN LENGTH (in.)
1	3.0	0.50	78	71.25
2	3.0	0.50	52	35.675
3	3.0	0.50	60	35.675
Web				
Width	6	inches		
Thickness	0.002	inches		
Modulus	600000	psi		
Material	Polyester			

Table 5-1: Details of the Rollers and the Web in Ahmad's experiments.

Ahmad's experimental set up installed in a continuous loop web transport machine is illustrated in Figure 5-2.

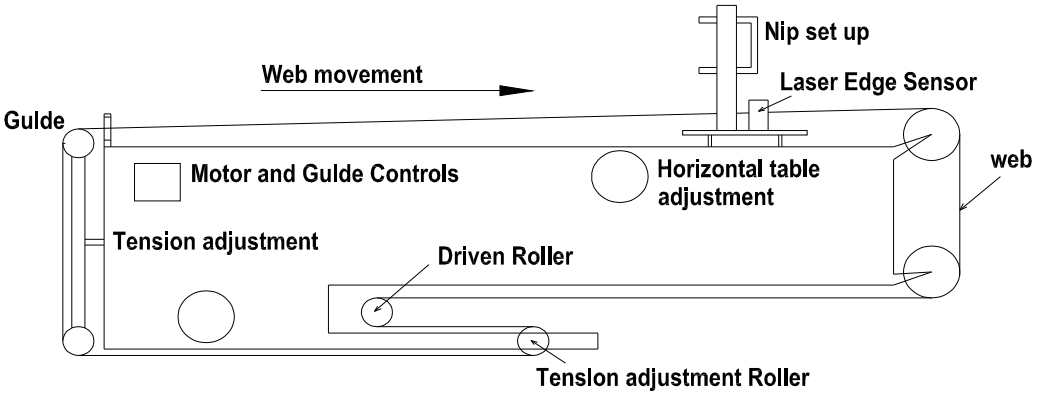

Figure 5-2: Ahmad's experimental set up in a continuous loop .

Load was applied on either side of the nip pneumatically by the cylinders shown in the picture. An uneven loading gave rise to the deflection of the polyester web as it passed through the nip of identical rubber covered rollers.

An edge sensor was used to measure the deflection of the web. This sensor used laser to detect the edge of the web. The resolution of the measurement technique used was 0.001 inches. The initial web tension was 5.4 pounds.

The web was centered in the nip and the nip was evenly loaded. Then the uneven loading condition was introduced by incrementing the load on one side. A simple schematic of the load application and the web deflection is shown in the Figure 5-3.

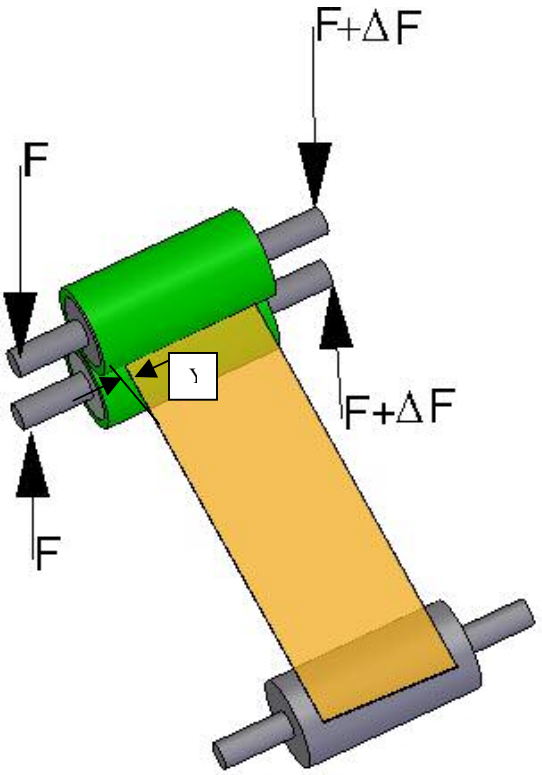

Figure 5-3: Uneven Load application and web deflection.

The deflection of the web was measured for each load increment. Three sets of data were taken for each set of rollers with the starting nip loads were 24.9, 49.86 and 74.79 lb on both sides of the nip. The experimental data thus obtained for the web deflections for varying nip loads is shown in Figure 5-4.

The variables used in the experiments of Ahmad will be used in Shelton ’s [15] expression to compute the theoretical deflection of the web. The theoretical deflections will be compared with that of the experimental deflections measured.

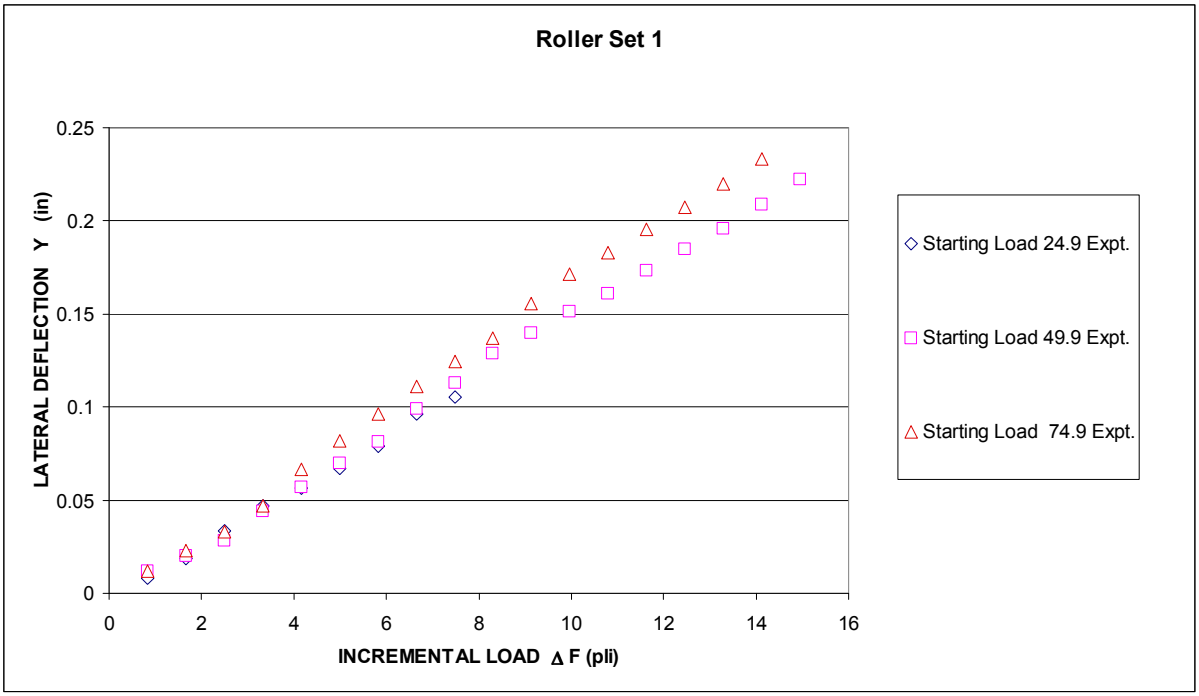

Figure 5-4: Ahmad's experimental data for roller set 1.

5. 3 NIPCODES:

Good [5] developed software codes for the force vs. deformation relations of the nip roller pairs. He addressed the contact problem in the nip between a metal roller and a rubber covered roller in his code called MRNIP. The contact problem in the nip between two identical rubber cover roller pairs is dealt with in his code called RRNIP. As this chapter deals with the lateral deflection of the web between two identical rubber-covered rollers, RRNIP will be discussed further.

RRNIP is an user interactive software program. The code requires inputs such as the dimensional details of the rollers and the web, material properties of the rollers and the web, and the input load on both the sides of the nip. All the

inputs given to the code are either readily available or measurable in a practical scenario. A typical set of identical rubber covered rollers with the metal core and the stub shafts for load application is shown in Figure 5-5.

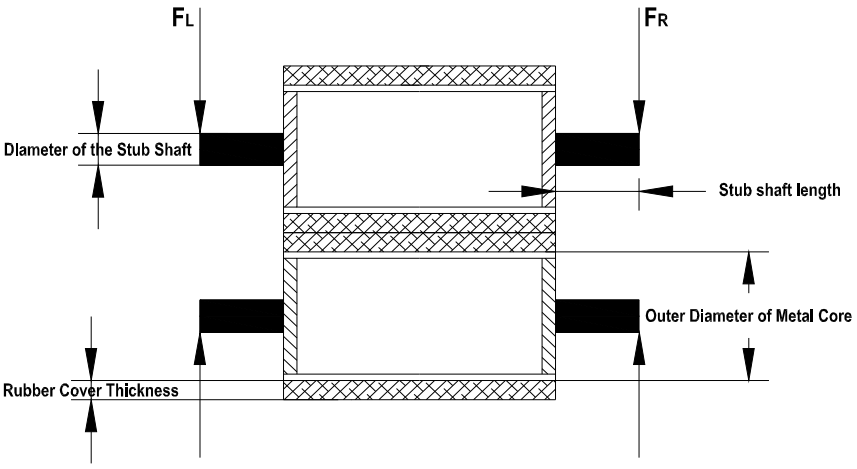

Figure 5-5: Details of the Identical Nip Roller pairs

A beam finite element model is used in combination with the Winkler foundation element to solve the problem. The rubber covered roller is divided into 10 finite beam elements. The stub shafts at either end of the roller where the load is applied are modeled as beam elements too. Thus the code divides the roller set up as 12 finite beam elements. The finite element formulation of the nip roller is represented in Figure 5-6.

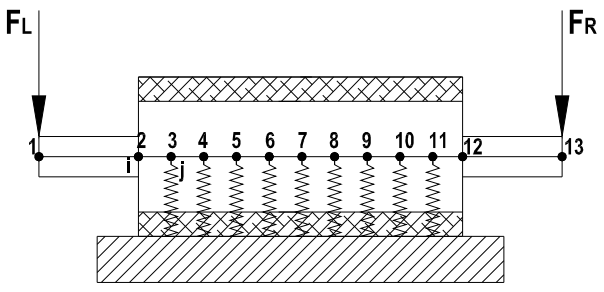

Figure 5-6: Finite Element Model of two identical Rubber covered rollers in contact.

A beam finite element is represented in Figure 5-7 with the nodes (i, j) and the degrees of freedom (v_1, θ_1, v_2, θ_2). This beam element is used to model the stub shaft and the metal core of the roller.

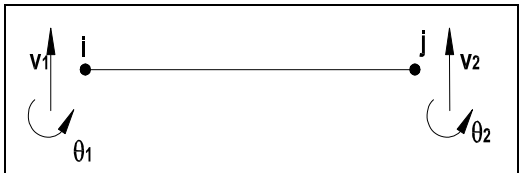

Figure 5-7: A finite beam element.

The stiffness matrix expression for a beam element loaded with concentrated moments at forces at its nodes is given by:

$$\begin{bmatrix} f_i \\ M_i \\ f_j \\ M_j \end{bmatrix} = \frac{EI}{L_e^{\,3}} \begin{bmatrix} 12 & 6L_e & -12 & 6L_e \\ 6L_e & 4L_e^{\,2} & -6L_e & 2L_e^{\,2} \\ -12 & -6L_e & 12 & -6L_e \\ 6L_e & 2L_e^{\,2} & -6L_e & 4L_e^{\,2} \end{bmatrix} \begin{bmatrix} v_i \\ \theta_i \\ v_j \\ \theta_j \end{bmatrix}$$

Equation 5-1

A Winkler foundation element is represented in Figure 5-8. Good used this element is used in modeling the rubber cover of the roller.

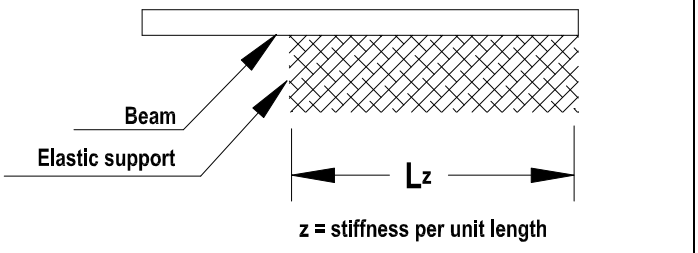

Figure 5-8: A Winkler foundation element.

The expression for the Winkler foundation element which is normally used to model the elastic foundation beneath a beam is given by:

$$\begin{bmatrix} f_i \\ M_i \\ f_j \\ M_j \end{bmatrix} = \frac{ZL_e}{420} \begin{bmatrix} 156 & 22L_e & 54 & -13L_e \\ 22L_e & 4L_e^{\,2} & 13L_e & -3L_e^{\,2} \\ 54 & 13L_e & 156 & -22L_e \\ -13L_e & -3L_e^{\,2} & -22L_e & 4L_e^{\,2} \end{bmatrix} \begin{bmatrix} v_i \\ \theta_i \\ v_j \\ \theta_j \end{bmatrix}$$

Equation 5-2

The stiffness of the elastic foundation 'Z' in Equation 5-2, which has the units of stiffness per unit length, is expressed by the theoretical force-deformation algorithm by K.L.Johnson.

$$Z = \frac{2}{3} \frac{(1-\nu)^2}{1-2\nu} \frac{E_c}{1-\nu^2} \frac{\sqrt{2R}}{t} \sqrt{v}$$

Equation 5-3

The stiffness of the beam and the Winkler elements are assembled into a global stiffness matrix G and a set of equations in the form {F} = [G] {v} is solved. Since Equation 5-3 for the stiffness requires deformation for computation, the whole set of equations is solved in iterative method. And the model solves the unknown deformations on the rubber cover.

RRNIP also gives the effective nip load acting at various points on the roller in the CMD, computed in the form of nodal loads. It also gives the variation of the rubber deformations, maximum pressure, Average Pressure and contact width in the CMD.

5. 4 Lateral deflection algorithm in RRNIP:

As discussed earlier, Shelton's [15] algorithm for lateral deflection of the web requires the change in web machine direction strain along the web width due to the velocity variation over the width. Hence, to incorporate the lateral deflection algorithm in RRNIP, the computation of the tangential strains becomes essential.

The deformations on the rubber cover due to the force applied are computed using finite element method in RRNIP, as explained earlier. The deformations thus computed are used as inputs for the tangential strain algorithms. It has been stated earlier that Good's [3] algorithm for the average tangential strain stands the best among the available closed form relationships. So, this algorithm will be incorporated in RRNIP.

To compare the performances of the Parish's and Shelton's tangential strain algorithms with Good's algorithm in the prediction of lateral deflection of the web, these algorithms are also used in RRNIP.

5.4.1 Parish's Algorithm:

Parish's algorithm for tangential strains vs. force applied is given by the Equation 2-35. It requires force applied, Poisson's ratio, Young's modulus of the rubber cover and half contact width as inputs.

RRNIP computes the effective force applied at each node of the finite beam element. Thus, the forces acting at various points along the CMD are known. Young's modulus for the rubber cover is given by Equation 2-3. This compression modulus depends on the rubber cover hardness, temperature and the strain rate. The rubber hardness and the process temperature remain constant in this expression. But, the strain rate varies as the load and, hence, the deformation varies. This leads to the variation in the values of Young's modulus at different points on the rubber cover along the CMD.

The strain rate required for the modified Young's modulus (given by Equation 2-3) is calculated as explained hereunder.

Strain rate has the units of (in./in)/sec. The web enters with a certain web velocity V fpm. The nip has a contact width 2a. The rubber cover has a thickness t. The deformation due to the applied load is δ. It can be noted that the deformation starts at zero at the beginning of the contact, attains a maximum value at the center of the contact and declines back to zero at the end. The value of the maximum deformation at the center of the contact zone is denoted by δ_{max} here for clarity. These quantities are explained in Figure 5-9.

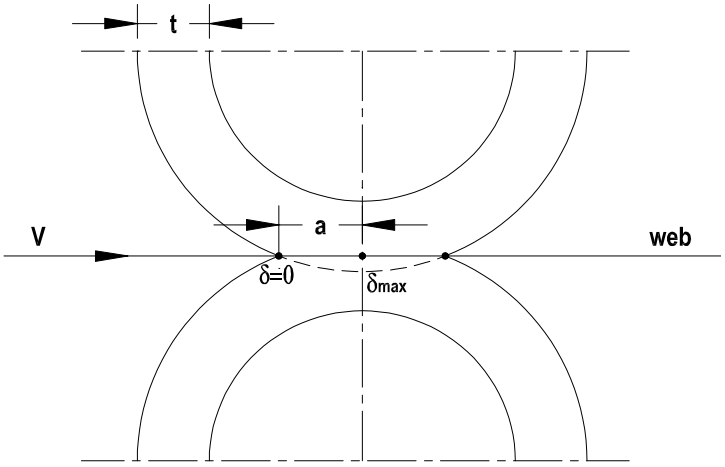

Figure 5-9: Illustration of the Variables in Strain rate calculation.

The deformation δ_{max} required for this calculation is generated from RRNIP. The contact width is calculated using this deformation in Equation 2-8. Strain rate can be expressed as:

$\dot{\varepsilon} =$ Strain / Time which has the units inch / inch / second.

Strain is expressed as $\frac{\delta_{max}}{t}$

The time required for the strain to vary from zero at the edge of the contact zone to $\frac{\delta_{\max}}{\mathrm{t}}$ is approximately the half width of contact (a) divided by the web velocity (V). This is expressed as Time = $\frac{a}{\mathrm{V}}$

Hence strain rate is computed by:

$$\dot{\varepsilon} = \frac{\frac{\delta_{\max}}{t}}{\frac{a}{V}}$$

Equation 5-4

RRNIP now gives the effective forces acting at various points along the CMD and also the half contact width and modified Young's modulus at these points. With these quantities as inputs, the tangential strain can be calculated as explained in CHAPTER 4. A typical result of the tangential strains on the rubber cover at the contact width using Parish's algorithm is shown in Table 5-2.

CMD Location	Load	Youngs modulus	Factor 1	Factor 2	strain
-4	18.993	684.461	0.098	0.154	0.015
-3.2	21.109	685.648	0.105	0.158	0.017
-2.4	23.303	686.760	0.113	0.161	0.018
-1.6	25.573	687.805	0.120	0.165	0.020
-0.8	27.920	688.792	0.127	0.168	0.021
0	30.342	689.728	0.134	0.170	0.023
0.8	32.836	690.616	0.141	0.173	0.024
1.6	35.403	691.462	0.148	0.176	0.026
2.4	38.041	692.270	0.155	0.178	0.028
3.2	40.748	693.043	0.162	0.180	0.029
4	43.522	693.784	0.169	0.182	0.031
Factor 1	$\frac{2F(1-\nu)}{\pi Ea}$	**Factor 2**		$(\psi(K,X))$	

Table 5-2: Parish's algorithm for Tangential strains.

5.4.2 Shelton's Algorithm:

Shelton's algorithm relates the tangential strains on the rubber cover to the deformations [1]. RRNIP computes the deformations due to the applied load at various locations along the CMD. These deformations are used as inputs in Shelton's expression (Equation 2-52). The velocity variations along the web width in the cross machine directions can be now computed.

5.4.3 Good's Algorithm:

Good's [3] algorithm also relates the tangential strains on the rubber cover to deformations. The average tangential strains are computed using Good's algorithm in the same way as it is done for Shelton's algorithm. The deformations computed by RRNIP are used as inputs.

A sample of the tangential strains computed by all the three algorithms, varying along the web width in the CMD are plotted for roller test case 3 with a starting load of 74.9 lb, in Figure 5-10.

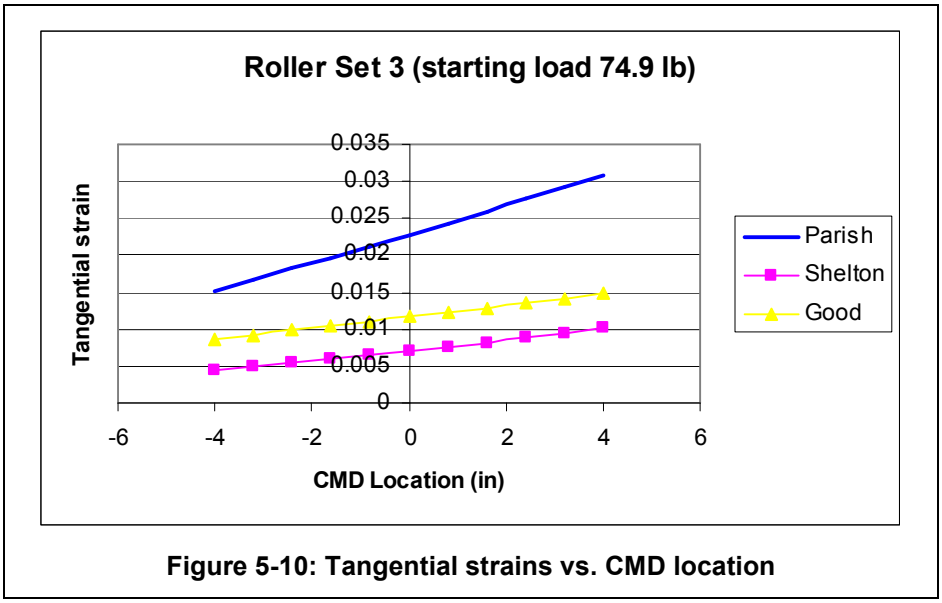

Figure 5-10: Tangential strains vs. CMD location

5. 5 Computation of Lateral Deflection of the web :

Shelton's [15] expression for lateral deflection (Equation 2-52) requires the value of the term $\Delta\varepsilon$, which is calculated for all the three algorithms. Applying this term to Shelton's equation, lateral deflections along the web at various positions in the machine direction (MD) are computed.

5.5.1 Computation of the change in strain over the web width ($\Delta\varepsilon$):

The term $\Delta\varepsilon$ is defined as the change in web MD strain over the web width due to the velocity variations over the CMD. It is computed from the tangential strains calculated at various locations along the CMD. The tangential strains vary along the web width because of the uneven loading and the velocity variations. The slope of this variation is multiplied with the web width to give the change in MD strain over the web width. This value is based on the maximum tangential strain that occurs in the center of the contact width. The effect of strains on the web will be maximum only at the center of the contact width. Hence, an approximate average value of $\Delta\varepsilon$ is computed by dividing the value by two. In simple terms, the computation of the term $\Delta\varepsilon$ can be stated as follows:

$$\Delta\varepsilon = \frac{d\left(\frac{\Delta V}{V}\right)}{dw} \bullet \frac{W}{2}$$

Equation 5-5

Where w is the roller width.

This term is calculated for all the three algorithms for each set of inputs in RRNIP. A sample calculation of the term $\Delta\varepsilon$ is as explained hereunder.

The tangential strains at various locations along the CMD of the rollers are calculated using the three different algorithms. A sample result of the calculation

using Parish's algorithm is listed in Table 5-2. These strains are obtained as the results for a certain set of input, which will be shown in Table 5-3 later in this chapter. The tangential strains for the same set of input, calculated using different algorithms are plotted in Figure 5-10. The variation of these strains is linear and the slopes of these lines are calculated. The slope calculated for each algorithm is multiplied by the web width and then divided by two, to get an average change in strain along the web width for this particular set of input. The change in strain calculated is used in further calculations of the lateral deflection of the web.

5.5.2 Computation of the term KK_{web}:

The constant KK_{web} in Shelton's expression for the lateral deflection of the web is defined as:

$$KK_{web}{}^{2} = \frac{T}{E_{web} I_{web}}$$

Equation 5-6

The web tension "T" is the sum of the input tension and the average tension in the web due to the applied forces.

$$T = T_{input} + T_{average}$$

Equation 5-7

and $T_{average} = \varepsilon_{average} \bullet E_{web} \bullet W_{web} \bullet t_{web}$

Equation 5-8

5.5.3 Computation of the lateral web deflection:

The term 'x' in Shelton's [15] algorithm for lateral deflection refers to the location in the web, in the MD. It starts at zero at the upstream roller and ends with the maximum value, the span length L, at the rubber covered rollers.

The span length of the web is divided by 10 and the lateral deflections at each of these locations are calculated. The starting load levels used in Ahmad's experiments are 24.9, 49.87 and 74.79 respectively. The same load levels are given as inputs for the load at the left end of the stub shaft. The loads at the right end are later increased in increments. A typical set of inputs given to RRNIP specifically for the lateral deflection computation is shown in Table 5-3.

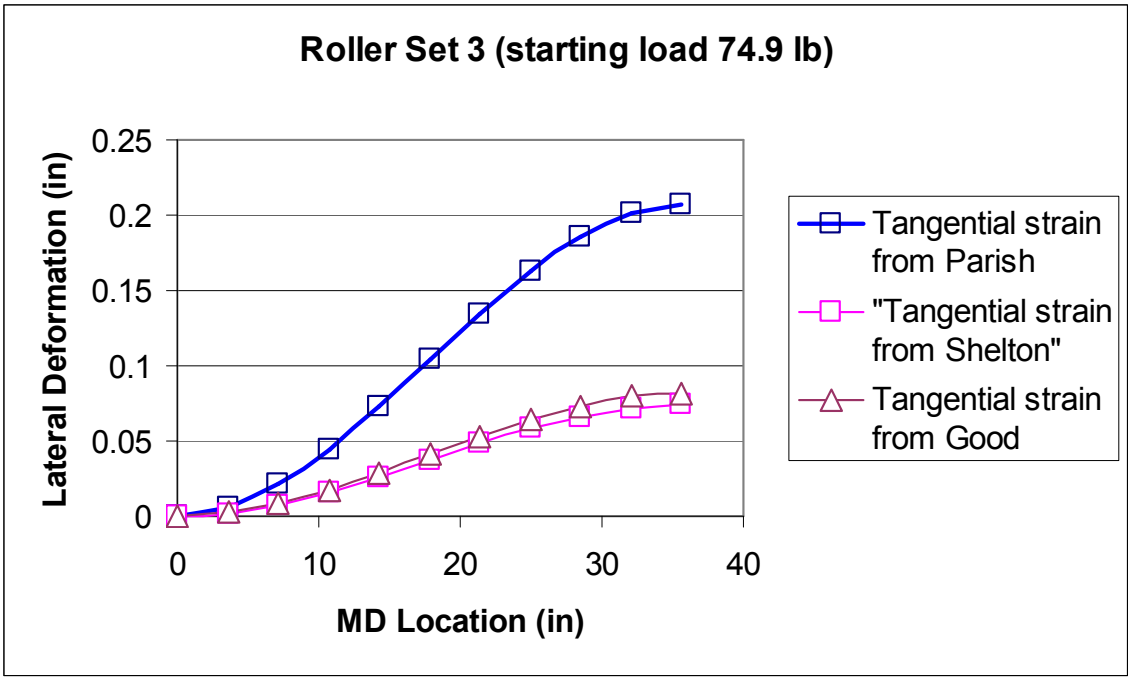

Figure 5-11: Lateral deflection of the web vs. MD location

The tangential strains and the term $\Delta\varepsilon$ are calculated for each set of inputs. Then, the lateral deflections in the web span at ten locations along the

MD are calculated. The variation of the lateral deflections along the web span is shown in Figure 5-11. This Figure shows the comparison of the results computed by all the three algorithms. This plot is generated for the sample inputs shown in Table 5-3.

Outer Roller Diameter, in.	3
Rubber Cover Thickness, in	0.5
Rubber Hardness, Shore A or IRHD	60
Nip Load Left, lb	74.9
Nip Load Right, lb	89.9
Web Velocity, fpm	10
Nip Roller Temperature (Celsius)	20
Width of Web, in	6
Length of Web Span, in	35.675
Web Thickness, in.	0.002
Modulus of Web, in	600000
Web Tension, lb	6

Table 5-3: Sample Set of inputs for the Lateral deflection calculation

The maximum Lateral deflection of the web occurs at the nip. Hence the value of lateral deflection calculated for the tenth location at the end of the span length gives the maximum lateral deflection. The maximum lateral deflection calculated for each set of load inputs is computed for each set of rollers used by Ahmad. This is repeated for all the three algorithms. The maximum lateral deflections varying with the incremental load are plotted for each algorithm. Figure 5-12 shows the comparison of the maximum lateral deflections computed by all the three algorithms with the experimental data of Ahmad for roller set 1. Similar comparisons for all the other roller sets are shown in APPENDIX C.

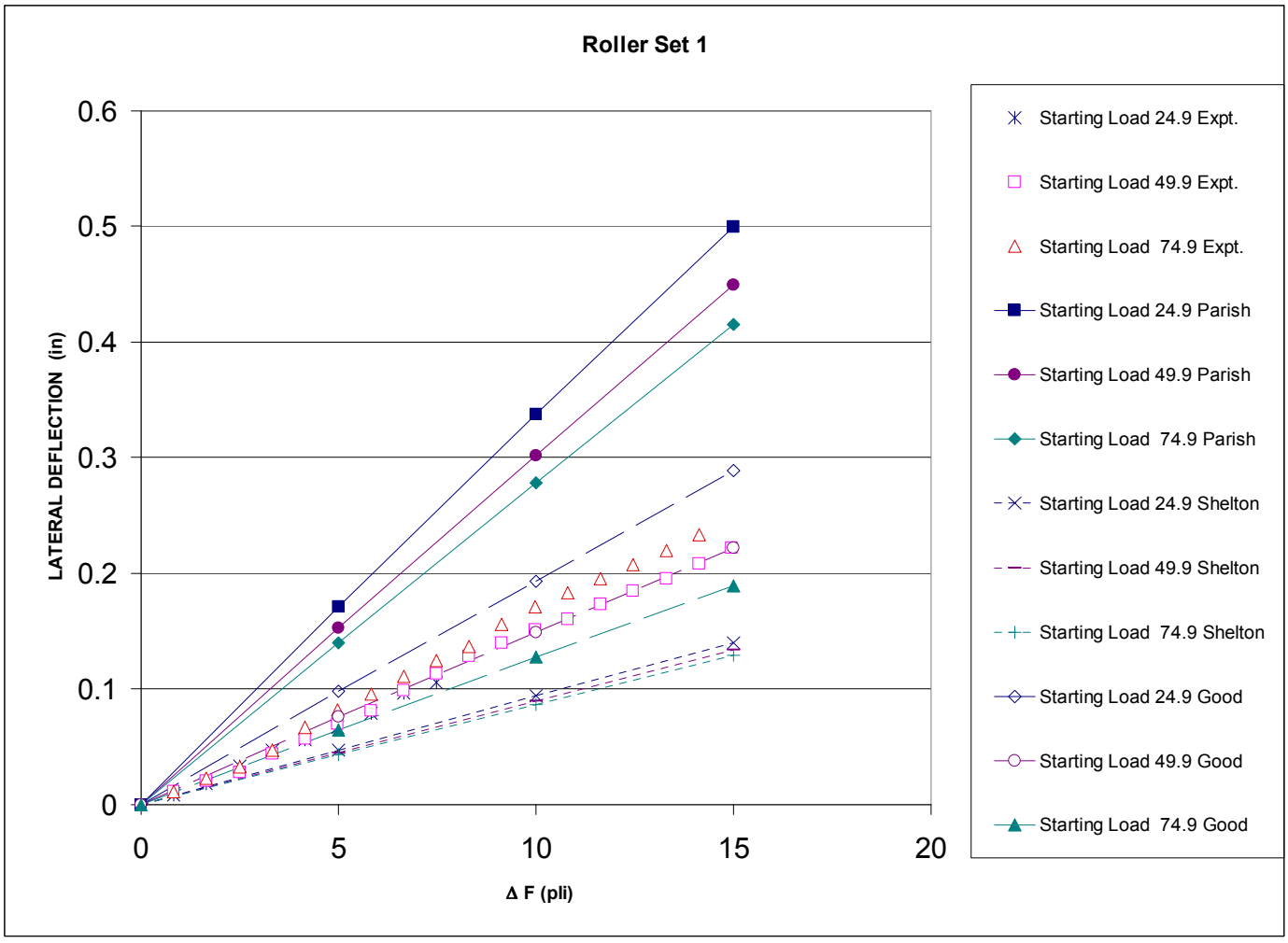

Figure 5-12: Comparison of Lateral Deflection Algorithms for roller Set 1.

5. 6 Analysis:

The maximum lateral deflection of the web is computed using Shelton's [15] algorithm by using the inputs for tangential strains from the algorithms of Parish, Shelton and Good. It has already been found out that Good's algorithm for tangential strain agreed the best. Yet, to further substantiate the finding, all the three algorithms are used in computing the maximum tangential strains.

An analysis, similar to the one explained in CHAPTER 3 and CHAPTER 4 is carried out in this case too, to find out the algorithm that best predicts the experimental data for maximum lateral deflection of the web.

The maximum lateral deflection of the web was computed for three levels of starting load for each roller set. A ratio of the theoretical result to that of the experimental data was computed for each level of the load increment. An average of these ratios is then computed for all the three sets of theoretical predictions using Shelton's expression, which use the inputs from the three tangential strain algorithms. This is repeated for all the nine sets of computations. A sample calculation is shown for roller set 1 with the starting load level of 74.79 lb in Figure 5-13.

Roller case 1	**Starting Load 74.9 expt**				**Ratios**		
Load Increment (lb)	Expt.	Parish	Shelton	Good	Parish/Expt	Shelton/Expt	Good/Expt
5	0.082	0.140	0.043	0.065	1.709	0.528	0.786
10	0.171	0.278	0.086	0.128	1.625	0.504	0.745
15	0.233	0.415	0.129	0.190	1.779	0.554	0.813
average ratio					1.704	0.529	**0.781**
Variation					0.704	0.471	0.219
	Minimum variation			**0.219**	**Good**		

Figure 5-13: Lateral web deflection---Computation of the Average Ratio

This average ratio shows which tangential strain algorithm gives better results with Shelton's lateral web deflection expression. For the case illustrated in Figure 5-13, Good's algorithm performs better with an average ratio of 0.7813. As stated in CHAPTER 3 and CHAPTER 4, the theory performs better if its average ratio is closer to 1.

To analyze the performance of all the theories, an Overall Average Ratio (OAR) is computed for all the nine different cases. The theory which has the OAR closer to 1 performs better in combination with the Shelton's Lateral web deflection expression. The result of the computation of the OAR is listed in Table 5-4.

Overall Average Ratio				
Roller Cases	**Starting Load Levels**	**Parish**	**Shelton**	**Good**
1	24.9	2.545	0.706	1.463
	49.9	2.067	0.613	1.023
	74.9	1.704	0.529	0.781
2	24.9	1.965	0.635	0.859
	49.9	1.400	0.500	0.553
	74.9	1.073	0.408	0.406
3	24.9	2.155	0.662	1.012
	49.9	1.601	0.537	0.669
	74.9	1.193	0.424	0.472
OAR		1.745	0.557	**0.804**
Variation		0.745	0.443	0.196
Minimum variation :		**0.196**	**Good**	

Table 5-4: Lateral web deflection--Computation of the overall Average Ratio

Good's model for the tangential strain in the rubber cover agrees best with the experimental model. It shows the Overall Average Ratio of 0.196. Hence, Good's theory for tangential strain performs better in predicting the lateral web deflection using Shelton's expression. The Tangential strain algorithm and the web deflection algorithm are included in RRNIP.

CHAPTER 6

CONCLUSIONS AND FUTURE WORK

6. 1 Summary:

The objective of this study was to quantify the lateral steering of a web due to a non-uniformly loaded nip of rubber covered rollers. The “best” available closed form relationships for the force vs. indentation and also for the force or indentation vs. tangential strain in the rubber cover were to be determined. The new expression for the compressive modulus of rubber developed by Good [6] at the Web Handling Research Center was to be incorporated in the force vs. indentation algorithms and the modified versions were to be studied. The lateral deflection of the web was to be computed using the inputs from these relationships. The algorithms for the computation of the tangential strain and the lateral web deflection were to be incorporated in the application software code RRNIP developed by Good [5].

The theoretical results of the available closed form relationships for the force vs. indentation algorithms were compared with Good’s experimental deformation data. K.L. Johnson’s algorithm modified with the new compression modulus yielded best results.

It could be noted that Johnson [9] and Lindley [10] made similar assumptions in their derivations for the force vs. deformation algorithms. They assumed that the load acting is being reacted by a rubber block whose width was equal to the width of the nip contact zone. Lindley [10] and Good [4] used a factor 'k' in their expressions, which takes the confinement of rubber into account. Evans [2] made an assumption of uniform external pressure acting on a rubber covered cylinder. The algorithm developed by Parish [12] and [14] was empirical. Miller 's [11] algorithm was based on Hannah's [7] and Parish's [14] work.

6. 2 Conclusions:

1. For the test cases studied, the best relationship for force versus indentation is Johnson's algorithm (Equation 2-12). At higher load levels, the confinement of the rubber becomes more prominent. Thus, as shown by Lindley [10], at these conditions, Johnson's algorithm might not prove the best.

2. The application of the new expression for compression modulus of the rubber, which is based on the strain rate, temperature and hardness of the rubber, yielded better results in all the test cases.

3. The closed form algorithms of Parish [13], Shelton [1] and Good [4] for the tangential strain in the rubber cover, were compared with Good's [4] experimental data. Parish's [12] algorithm included an empirical method for determining the nip contact width to determine the tangential strain. Shelton's [1] expression was also empirical. Good's [3] algorithm (Equation 2-44) was found to be the "best".

4. In order to determine the lateral deflection of the web, the results from Johnson's modified algorithm were used for the force vs. indentation relation. Good's [3] algorithm for the tangential strain vs. indentation could be used as an input to the lateral deflection algorithm. But, in order to substantiate the finding, all the three algorithms for the tangential strains were tried. The lateral deflections thus computed were compared with Ahmad's [1] experimental data. Shelton's expression for the lateral deflection yielded best results with Johnson's [9] modified algorithm for force vs. indentation and Good's [3] algorithm for the tangential strain as inputs. This model can be used for the prediction of the lateral steering in an unevenly loaded nip.

6. 3 Future Work:

The closed form relationships for the force vs. indentation relationships should be verified for higher load levels. As mentioned earlier, the rubber confinement effect would become important at higher loads and Johnson's algorithm might not be the best in those conditions.

The velocity of the rubber cover in the nip contact zone is greater than the velocity of the cover outside the contact zone. A theory which could predict this would yield a better relationship between the tangential strain and the force or indentation. A model which would include the web in predicting the tangential strain relationships would also be beneficial.

It was noted that with increasing load levels, Ahmad's [1] experimental data showed an increase in the trends of lateral deflection for all the roller test cases, while the theoretical models predicted a decreasing trend. The tangential

strain that occur on the rubber covers in the nip contact zone is not equal to the tangential strain experienced by the web that transits between the rollers. This is due to the difference in the stiffness of the rubber and the web material. The study on the effect of friction between the rollers and the web would provide better results in predicting the velocity variation and the lateral web deflection.

This work should also be extended for the nip between a rubber covered roller and a metal roller with webs made of different materials.

REFERENCES

[1] Ahmad, M.N., “Lateral deflection of a web due to a differentially loaded nip”, M.S. Thesis, Oklahoma State University, 1997.

[2] Evans, I., “The Rolling Resistance of a Wheel with a Solid A Rubber Tyre”, British Journal of Applied Physics, V.5, 1954, pp.187-188.

[3] Good, J.K., Proceedings of the WHRC Semi Annual Technical Review and Industrial Advisory Board meeting, Oct. 1999.

[4] Good, J.K., Proceedings of the WHRC Semi Annual Technical Review and Industrial Advisory Board meeting, Jun. 2001.

[5] Good, J.K., “Modeling Rubber Covered Nip Rollers in Web Lines”, Proceedings of the sixth International Conference on web Handling, 2001.

[6] Good, J.K., Proceedings of the WHRC Semi Annual Technical Review and Industrial Advisory Board meeting, Jun. 2005.

[7] Hannah, M., “contact Stress and Deformation in a thin Elastic Layer”, Quarterly Journal of Mechanics and Applied Mathematics, V.4, 1951.

[8] Hergenrether, M.C., “Investigations of Models for predicting deformation and strain in rubber covered nip rollers”, M.S. Thesis, Oklahoma State University, 2004.

[9] Johnson, K.L., Contact Mechanics, Cambridge University Press, 1989, pp.139-140

[10] Lindley, P.B., “Load-compression Relationships of Rubber units”, Journal of Strain Analysis, V.1, No.3, pp.190-195.

[11] Miller, R.D.W., “Variations of line pressure and rolling speed with indentation of covered rollers”, British Journal of Applied Physics, V.15, 1964

[12] Parish, G.J., “Measurements of pressure distribution between metal and rubber covered rollers”, British Journal of Applied Physics, V.9, Apr. 1958

[13] Parish, G.J., “Apparent slip between metal and rubber-covered pressure rollers”, British Journal of Applied Physics, V.9, Nov. 1958

[14] Parish, G.J., “Calculation of the behavior of rubber-covered pressure rollers”, British Journal of Applied Physics, V.9, Jul. 1961

[15] Shelton, J.J., “Lateral dynamics of a moving web”, Ph.D Dissertation, Oklahoma State University.

APPENDIX A

COMPARISON OF THE FORCE vs. INDENTATION ALGORITHMS

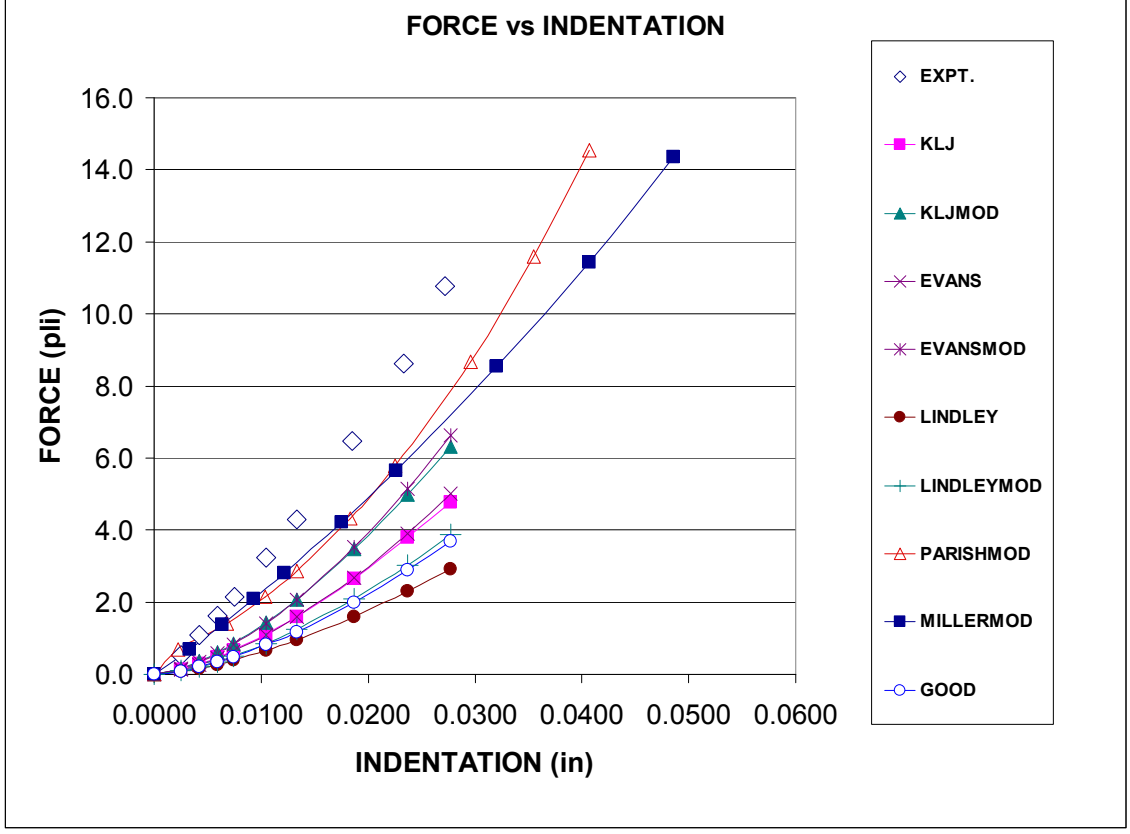

Figure A-1: Force vs. indentation for roller case 1.

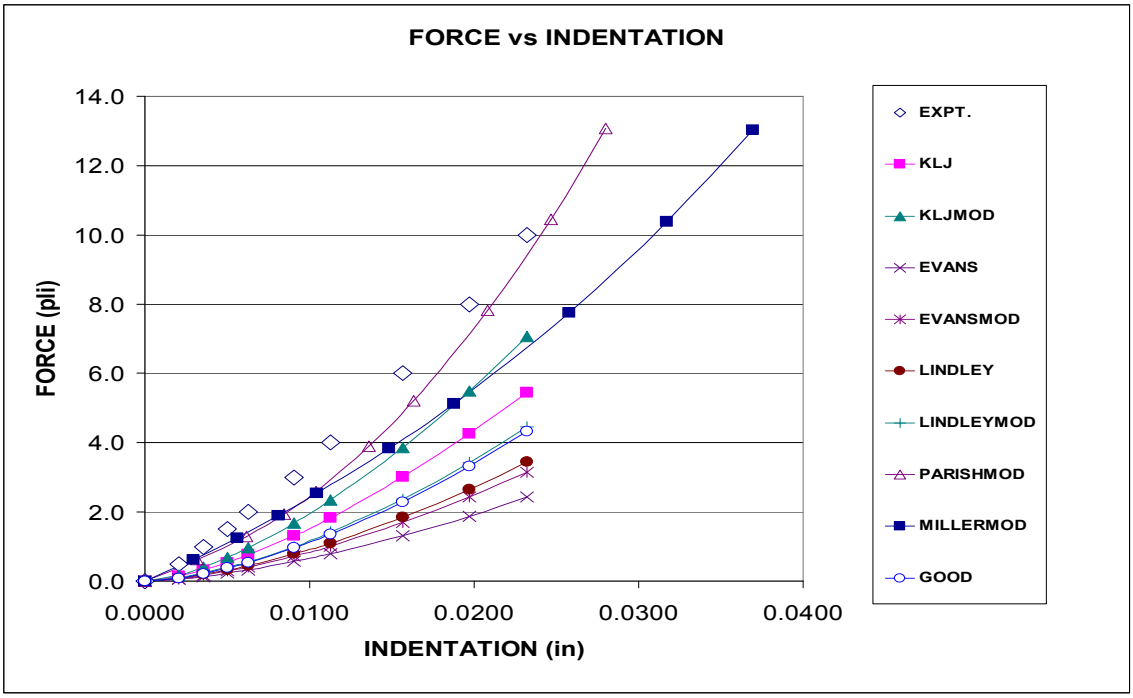

Figure A-2: Force vs. indentation for roller case 2.

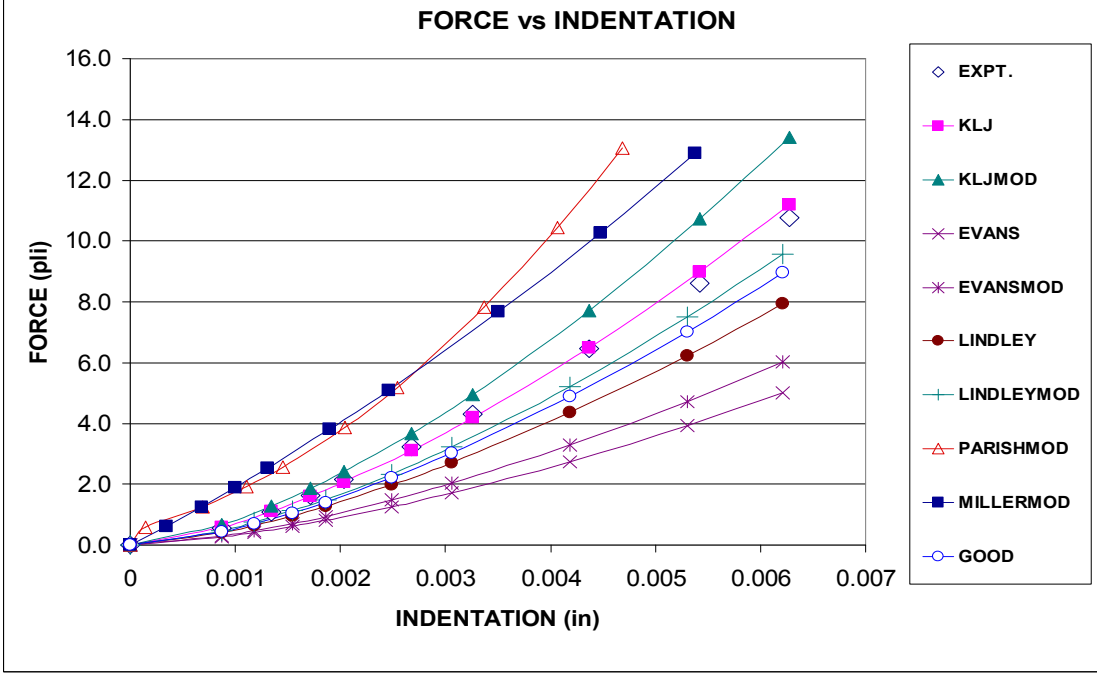

Figure A-3: Force vs. indentation for roller case 3.

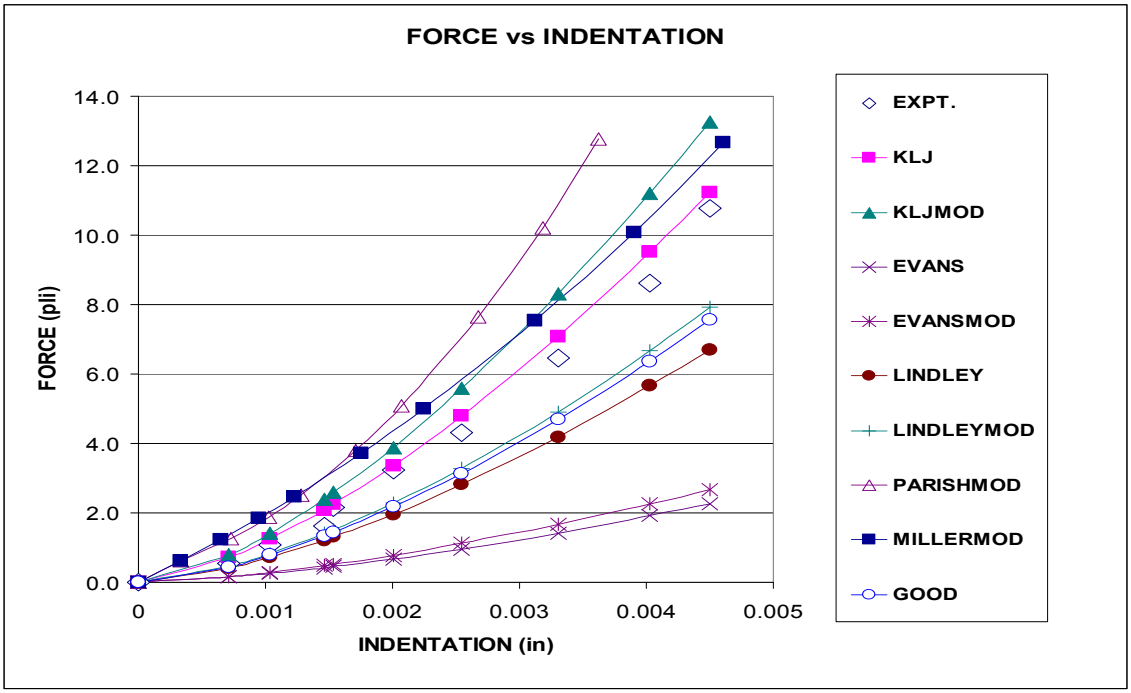

Figure A-4: Force vs. indentation for roller case 4.

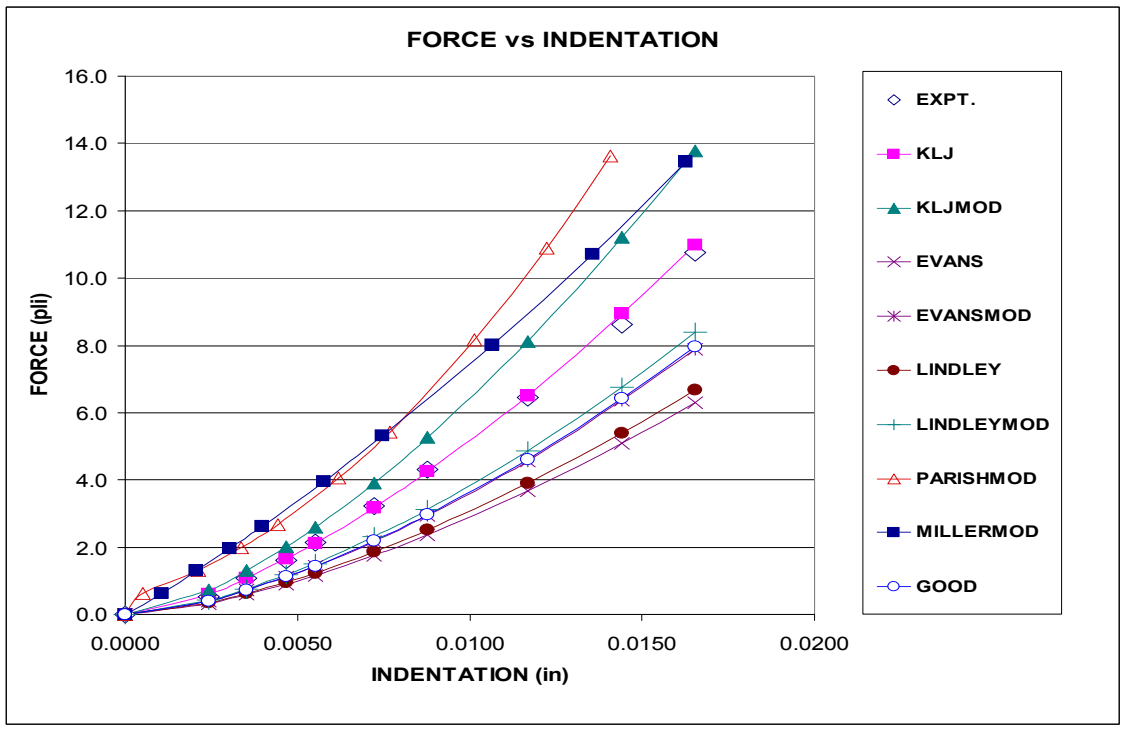

Figure A-5: Force vs. indentation for roller case 5.

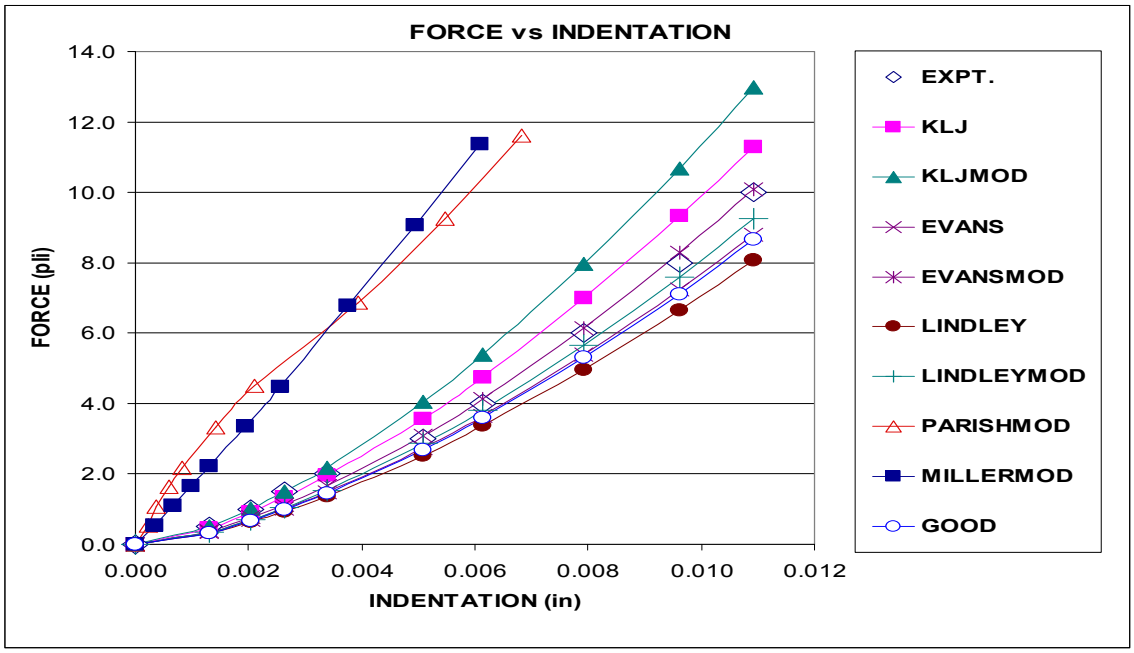

Figure A-6: Force vs. indentation for roller case 7.

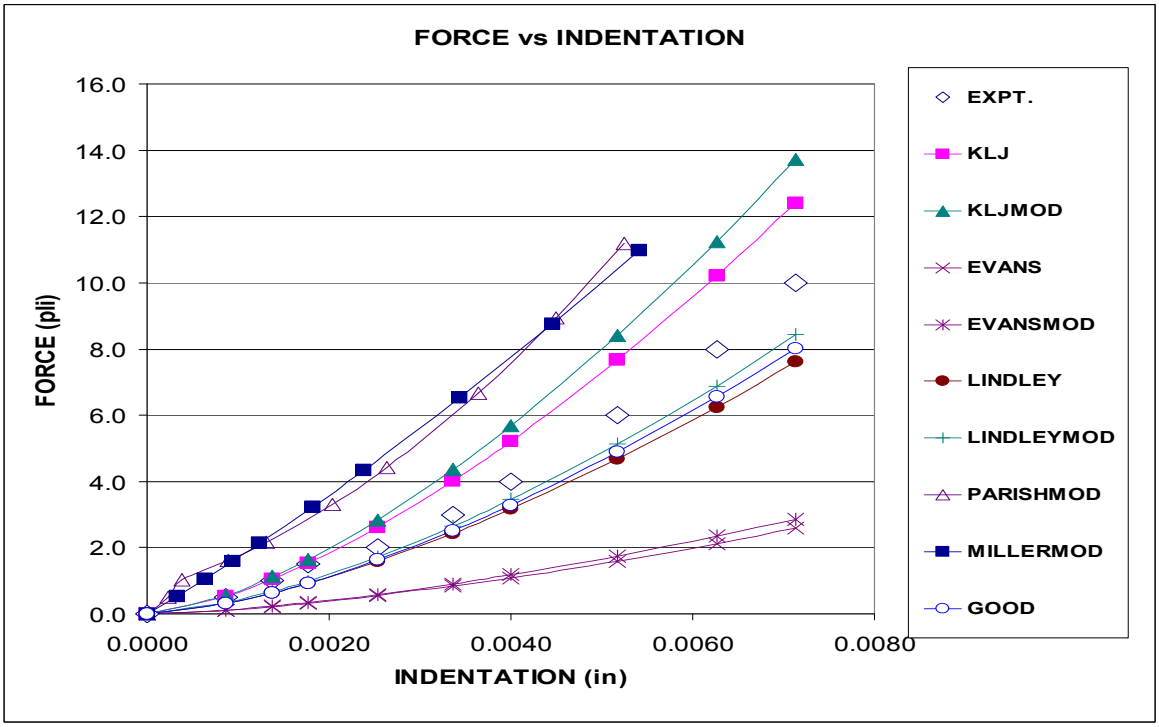

Figure A-7: Force vs. indentation for roller case 8.

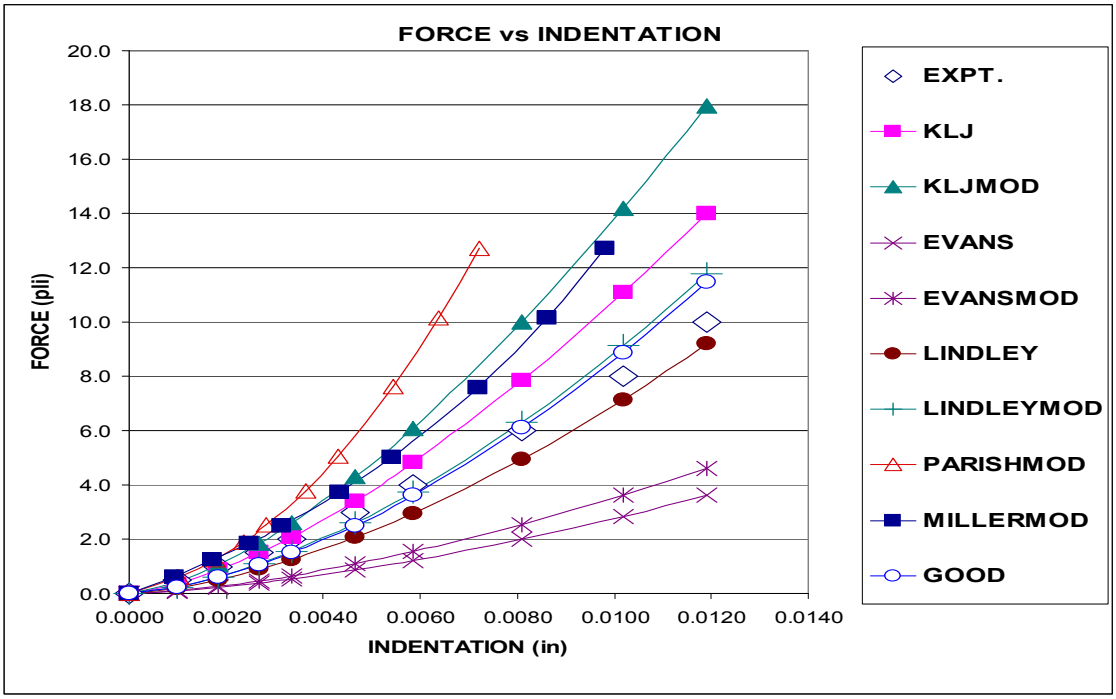

Figure A-8: Force vs. indentation for roller case 9.

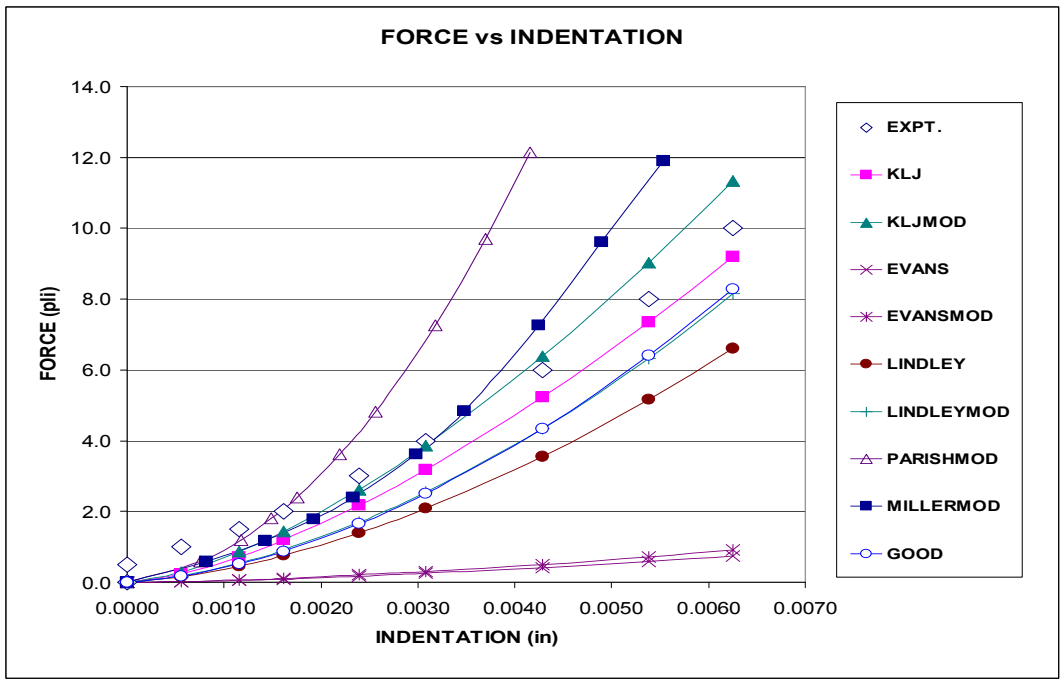

Figure A-9: Force vs. indentation for roller case 10.

APPENDIX B

COMPARISON OF THE TANGENTIAL STRAIN vs. LOAD / INDENTATION ALGORITHMS

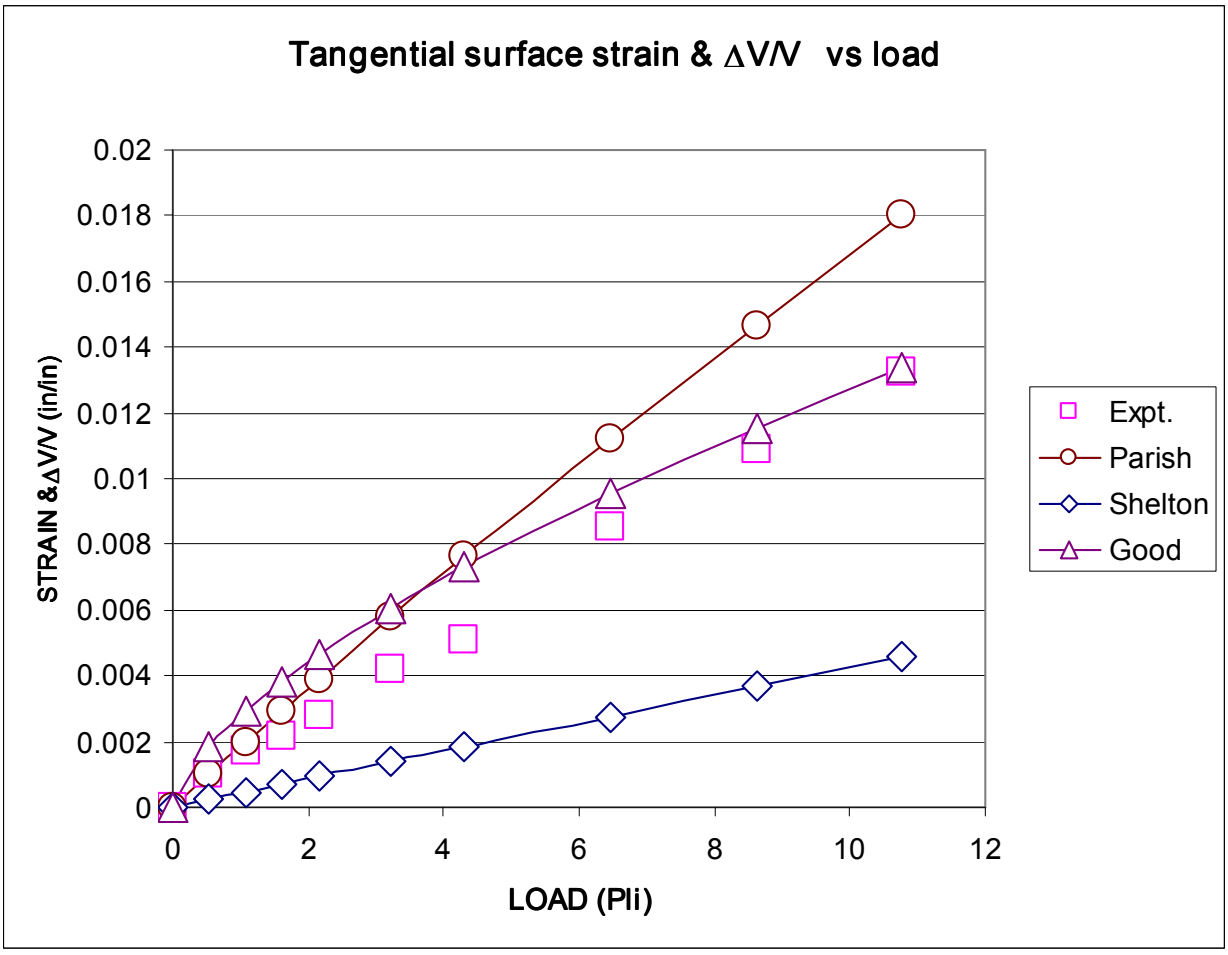

Figure B-1: Tangential Strain vs. Load / indentation for roller case 1.

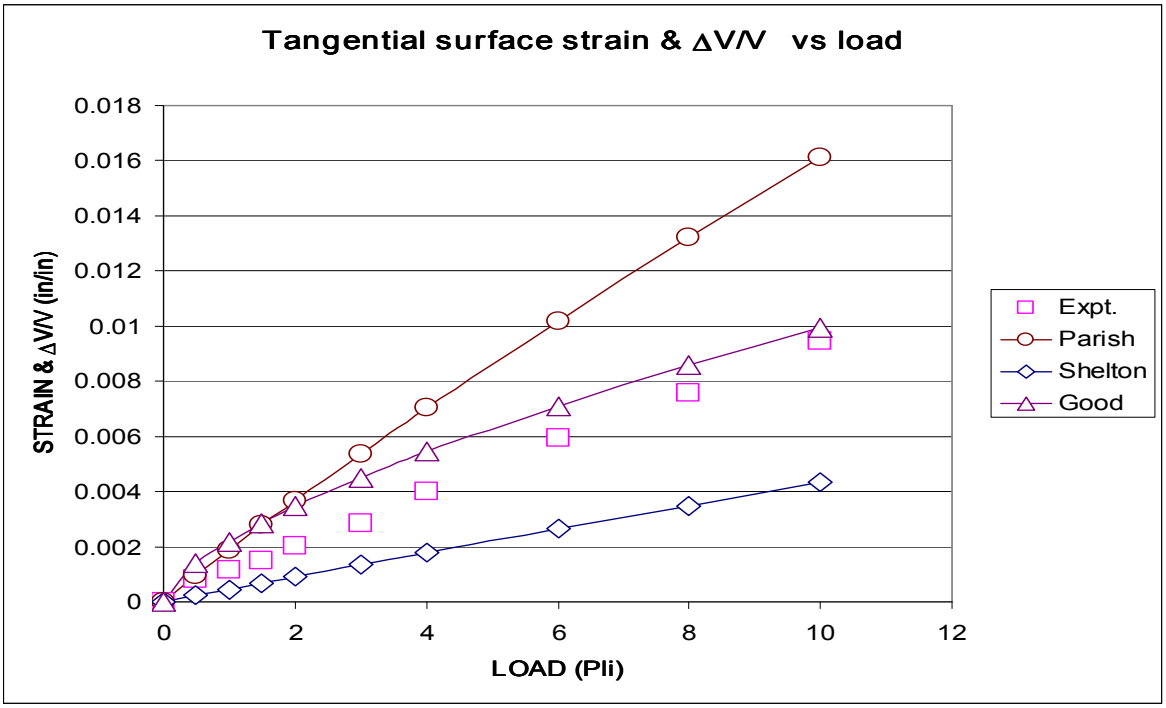

Figure B-2: Tangential Strain vs. Load / indentation for roller case 2.

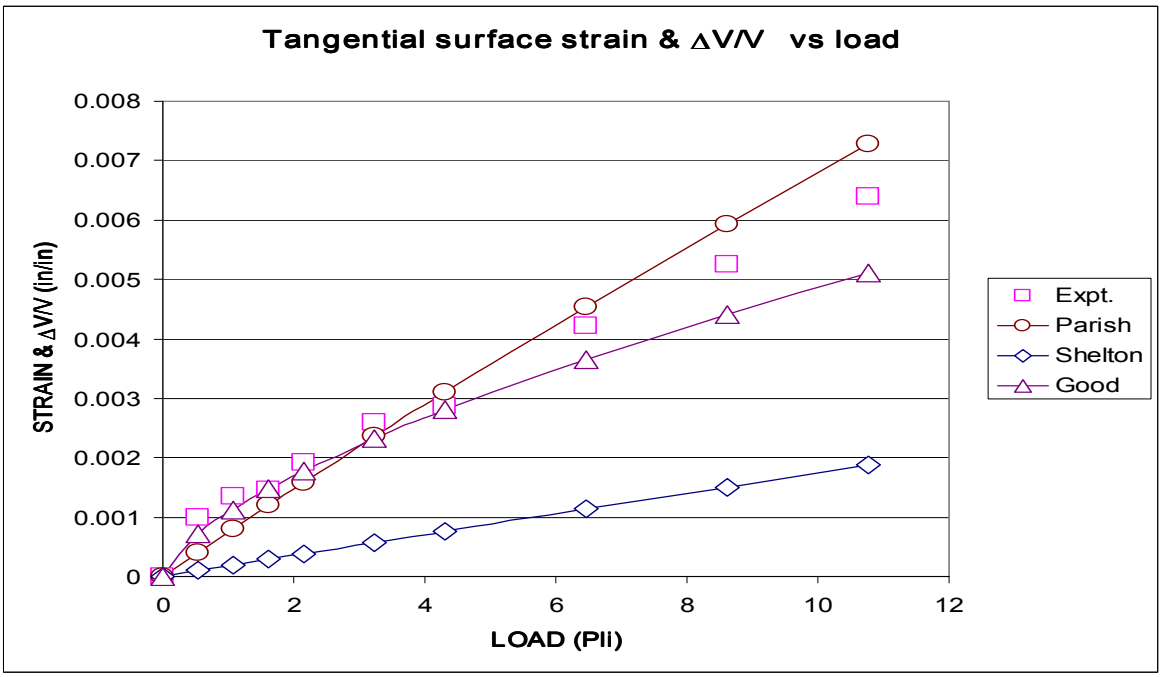

Figure B-3: Tangential Strain vs. Load / indentation for roller case 3.

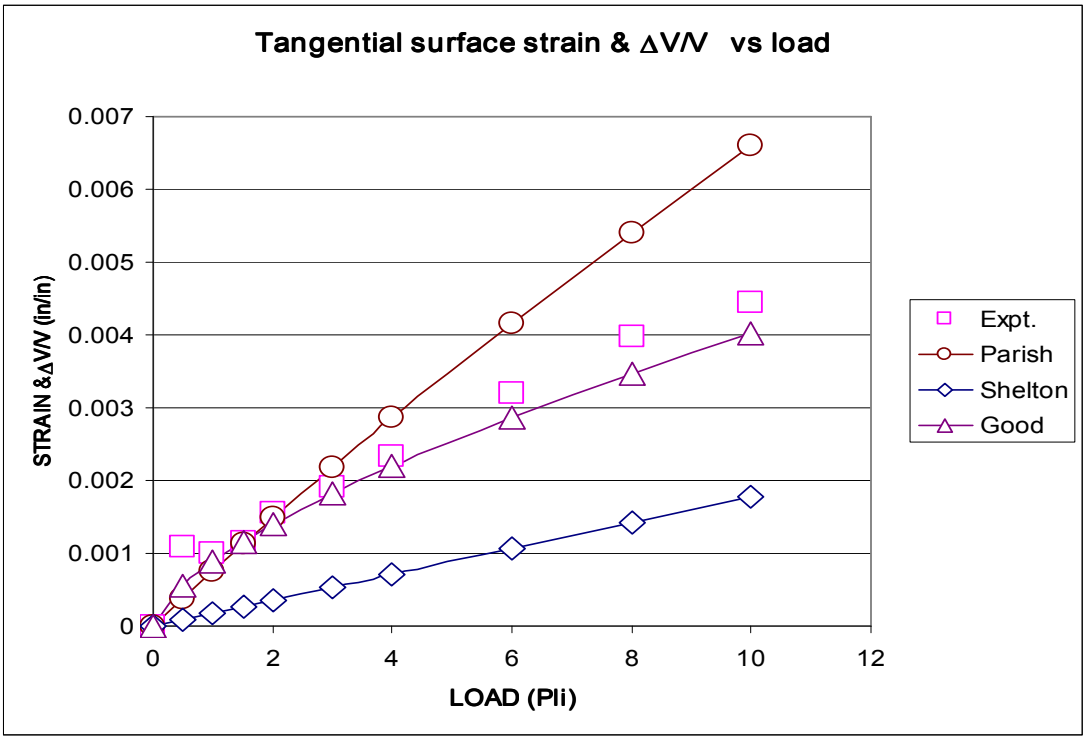

Figure B-4: Tangential Strain vs. Load / indentation for roller case 4.

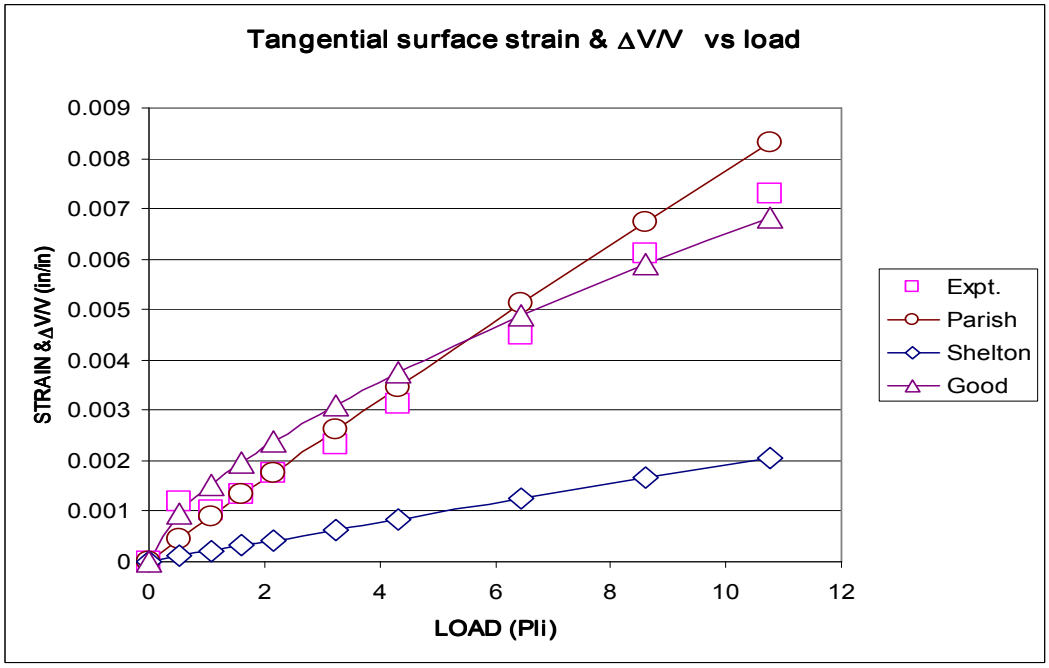

Figure B-5: Tangential Strain vs. Load / indentation for roller case 5.

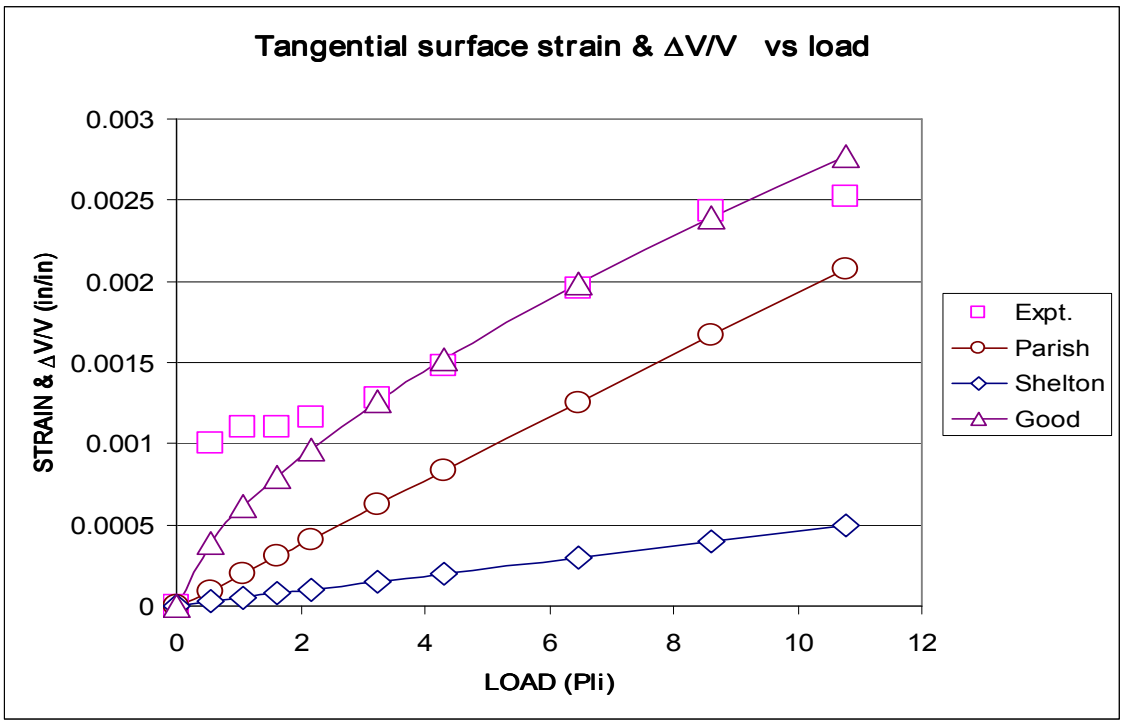

Figure B-6: Tangential Strain vs. Load / indentation for roller case 7.

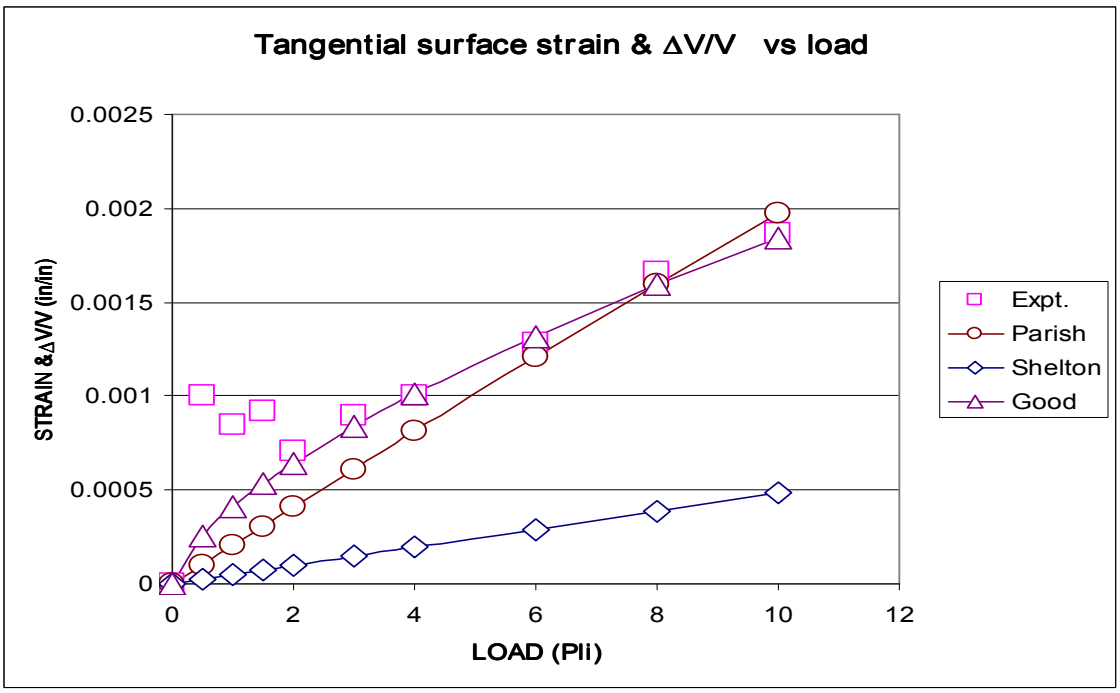

Figure B-7: Tangential Strain vs. Load / indentation for roller case 8.

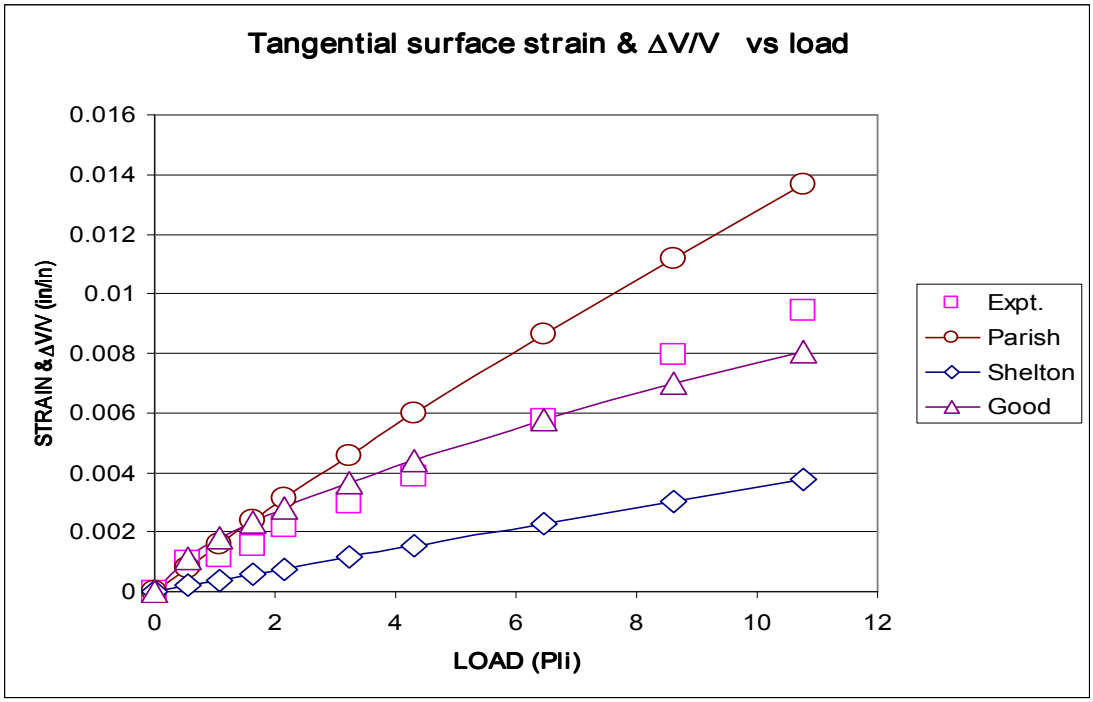

Figure B-8: Tangential Strain vs. Load / indentation for roller case 9.

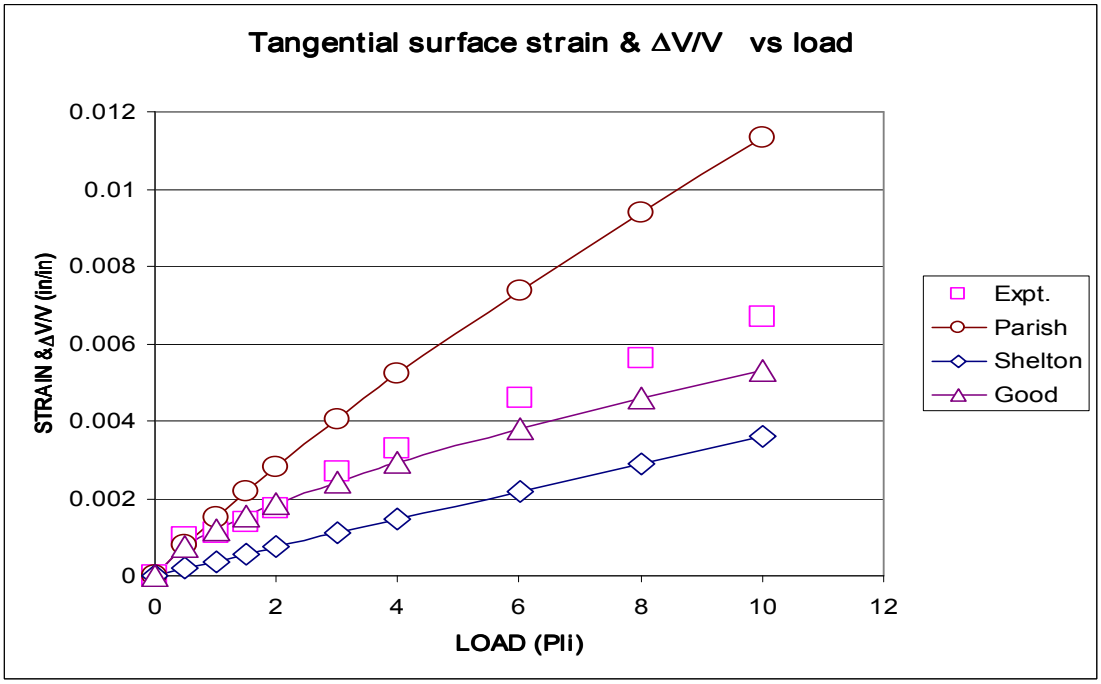

Figure B-9: Tangential Strain vs. Load / indentation for roller case 10.

APPENDIX C

COMPARISON OF LATERAL DEFLECTION ALGORITHMS

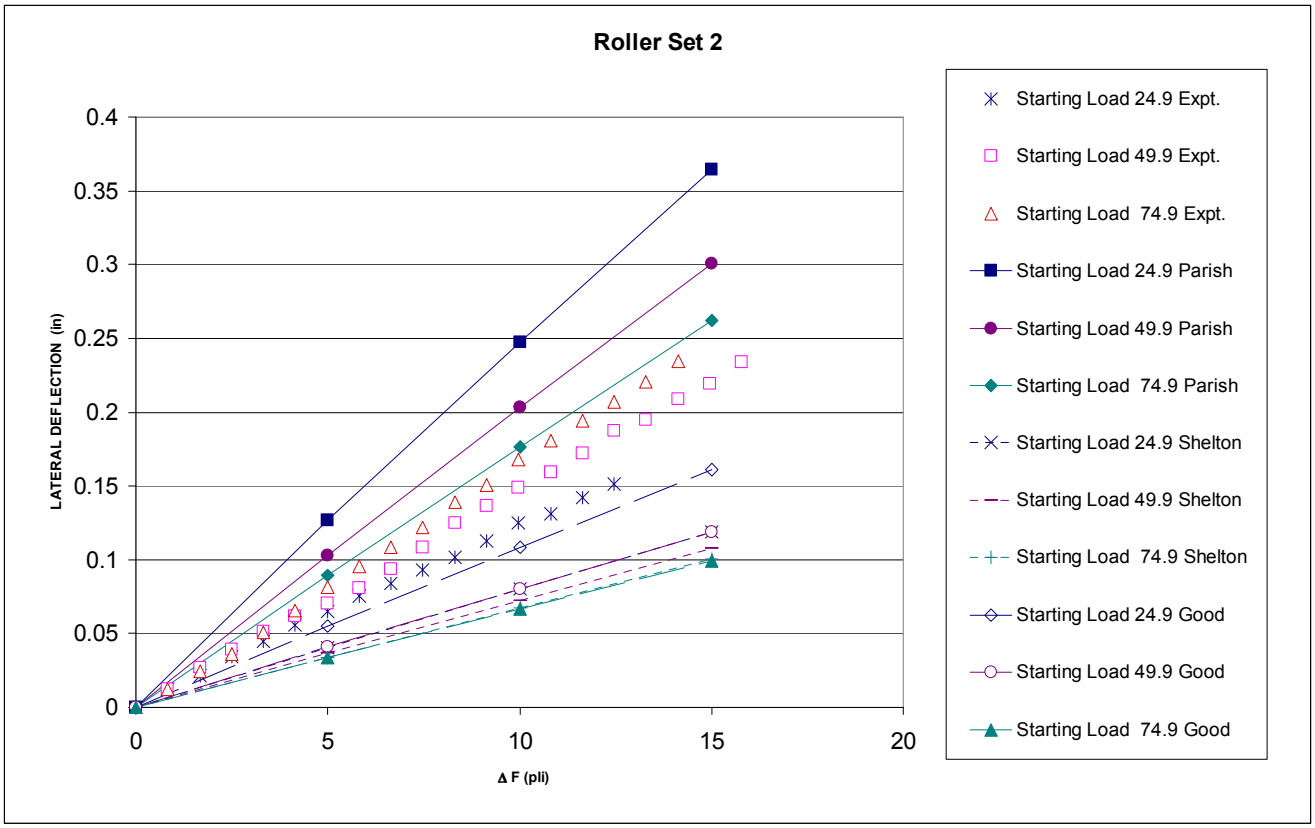

Figure C-1: Lateral deflection of the web vs. Incremental Load for roller set 2.

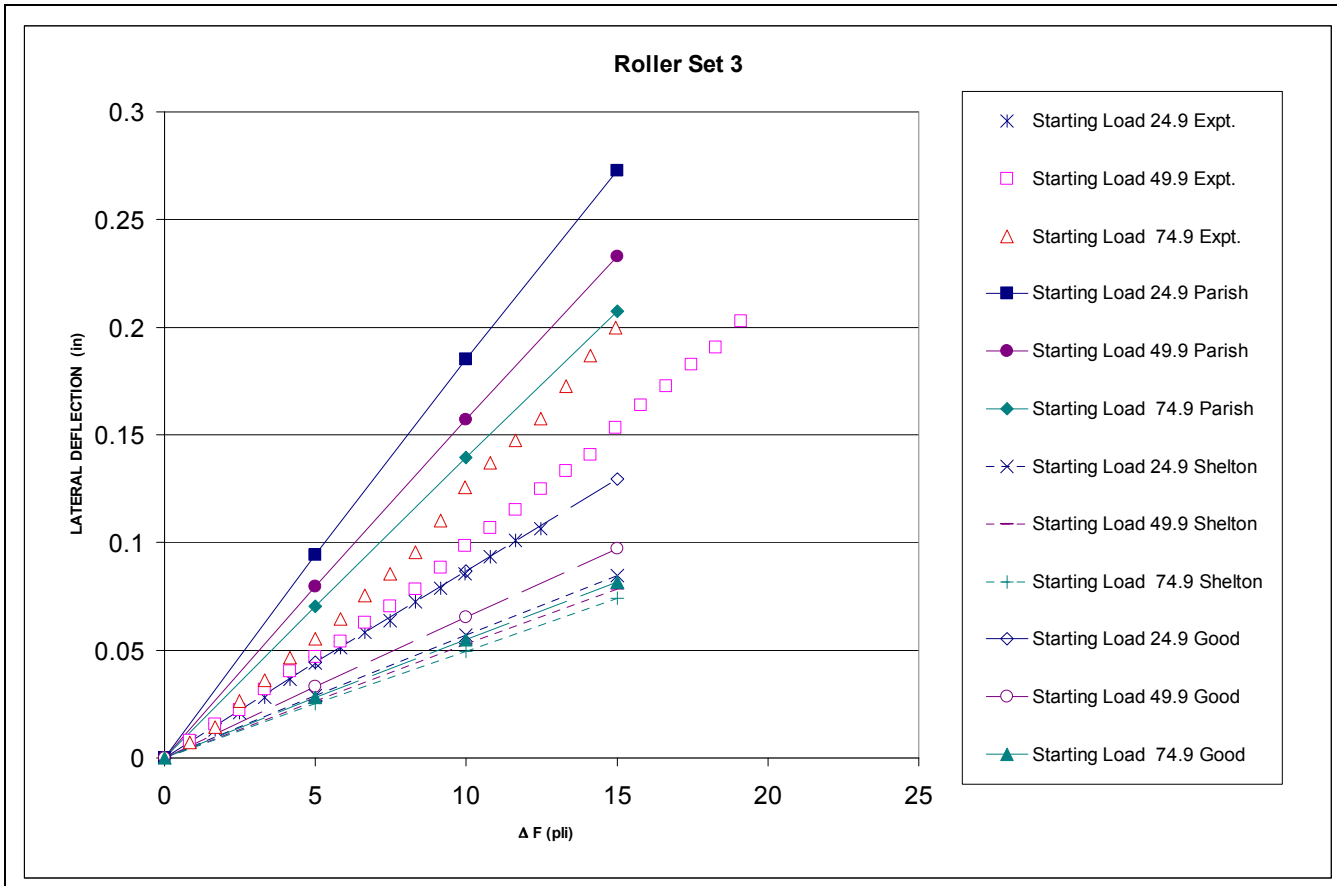

Figure C-2: Lateral deflection of the web vs. Incremental Load for roller set 3.

VITA

KAVITHA BALAIYAN

Candidate for the degree of

Master of Science

Thesis: LATERAL STEERING OF THE WEB IN A DIFFERENTIALLY LOADED NIP OF RUBBER COVERED ROLLERS.

Major Field: Mechanical Engineering

Biographical:

Personal Data: Born in Mannargudi, Tamil Nadu, India, on April 4, 1979, the daughter of Mr.T.Balaiyan and Mrs. B.Thavamani.

Education: Graduated from St. Mary's Girls' Higher Secondary school, Chengalpattu, Tamil Nadu, India, in May 1996;
Received Bachelor of Engineering Degree in Mechanical Engineering from College of Engineering, Guindy, Anna University, Chennai, India in May 2000;
Completed requirements for the Master of Science Degree with a major in Mechanical Engineering at Oklahoma State University in December 2005.

Professional Experience: Graduate Research Assistant, Department of Mechanical Engineering, Oklahoma State University, May 2004 to July 2005;
Deputy Engineer, Product Design Group, Naval Systems, Bharat Electronics Limited, (A Government of India firm, Ministry of Defence), May 2000 to January 2004.

Professional Membership: American Society of Mechanical Engineers.

Name: Kavitha Balaiyan Date of Degree: December, 2005

Institution: Oklahoma State University Location: Stillwater, Oklahoma

Title of Study: LATERAL STEERING OF THE WEB IN A DIFFERENTIALLY LOADED NIP OF RUBBER COVERED ROLLERS.

Pages in Study: 85 Candidate for the Degree of Master of Science

Major Field: Mechanical Engineering

Scope and Method of Study:

An unevenly loaded nip of rubber covered rollers can induce lateral deflection of the web. Closed form algorithms which relate the

(i) applied nip force to rubber cover indentations and

(ii) tangential strains on rubber cover to force/indentations

were verified. The algorithm which best predicted the experimental data in each case was chosen. The theoretical web deflection was determined using these algorithms as inputs and was compared with the experimental data. A new expression for compression modulus of rubber, developed by Good was used.

Findings and Conclusions:

K.L.Johnson's algorithm for force vs. indentation, modified with the new compression modulus yielded best results for the roller and load ranges in the experiments. Good's algorithm for tangential strain in the rubber cover was found to be the "best". Shelton's expression for lateral deflection of the web yielded best results with Johnson's modified algorithm for force vs. indentation and Good's algorithm for tangential strain as inputs.

ADVISOR'S APPROVAL: Dr. James Keith Good